SYSTEM PLANNING CORPORATION

MATERIALS PROCESSING THRESHOLD REPORT

1. Semiconductor Crystals for Infrared Detectors

FINAL REPORT

SPC 564

February 1980

Earl V. Sager
Terence R. Thompson
Robert G. Nagler

Prepared for
National Aeronautics and Space Administration
George C. Marshall Space Flight Center
Marshall Space Flight Center
Alabama 35812

SYSTEM PLANNING CORPORATION
1500 Wilson Boulevard • Suite 1500 • Arlington, Virginia 22209 • (703) 841-2800
Systems Research & Engineering Division

SPC Log No. 80-2022
Copy

MATERIALS PROCESSING THRESHOLD REPORT
I. Semiconductor Crystals for Infrared Detectors

FINAL REPORT
SPC 564

February 1980

Earl V. Sager
Terence R. Thompson
Robert G. Nagler

Prepared under
Contract NAS8-33554

Sponsored by
National Aeronautics and Space Administration
George C. Marshall Space Flight Center
Marshall Space Flight Center
Alabama 35812

CONTENTS

I. EXECUTIVE SUMMARY

A. INTRODUCTION

In 1978, System Planning Corporation (SPC) conducted a survey[1] for NASA of defense-related materials research activities ongoing within the Department of Defense and private industry. The purpose was to determine the prime areas of materials research and to find out if researchers had given thought to materials processing in space. The outcome of the survey was to isolate specific areas in which ultimate materials performance was not currently achievable and which might be improved by processing in the zero gravity environment of space. Based on that survey, NASA selected SPC to study in depth one or more of the promising areas of materials research. The purpose of the study was to look further into the possible benefits of materials processing in space and to devise a presentation by which NASA could generate interest on the part of DOD agencies in conducting materials processing experiments on future Space Shuttle scientific missions. The results of the study are documented in this report.

B. BACKGROUND

The short-term prospects for materials processing in space include its use as a research tool and in some rare instances its capability to provide sufficient material for practical uses. It was felt that initially, at least, this effort would be most profitably directed towards a material for which both possibilities exist. For this reason, semiconductor infrared

[1] J. W. Whybrew, et al., Analysis of Materials Processing in Space, SPC 390, November 1978.

detector materials, which are coming into rapidly increasing demand but which are very low mass production items, seemed to be a suitable choice.

The project began with an extensive search of the open literature pertaining to infrared detectors to determine what constitutes a good detector and in what way performance is limited by specific material properties. Continuing further, one could ask how the material property is related to aspects of processing and how undesirable characteristics might be eliminated. With a basic understanding of the subject in hand, interviews were conducted with a number of experts in the field to assess their perceptions of the state of the art and of the utility of zero-gravity processing. Based on this information base and on a review of NASA programs in crystal growth and infrared sensors, we have reassessed NASA program goals and have made suggestions as to possible joint and divergent efforts between NASA and DOD.

C. FINDINGS

1. Our conclusions as to the status of IR detector research are summarized below.

- The primary effort in IR detector materials is directed toward the development of HgCdTe alloys as a reliable and versatile material for producing multielement focal plane arrays. This material has the potential for satisfying nearly all the strategic and tactical military needs for infrared sensing and imaging.
- The need for high-quality HgCdTe crystals is currently expanding at a geometric progression and can be expected to increase even faster if techniques are devised to increase reliability and lower cost.
- There is a serious lack of physical knowledge from which to devise a comprehensive theory that can relate material processing technology to device performance. The production of HgCdTe crystals and other high-performance IR detector materials is based on recipes that have slowly evolved over the years. The basic information describing successful procedures is kept secret for commercial proprietary interests.
- Research programs currently exist for studying the thermodynamic behavior and defect chemistry of HgCdTe. Further funding is necessary to complete a framework of understanding from which reliable procedures for crystal growth can evolve. This funding is not

likely to originate with the commercial suppliers of IR crystals and devices.

- A role for space processing of IR crystals cannot now be properly determined because of the inconsistencies in the results of ground-based research. Fundamental research on ground-based crystal growth facilities is needed in order to quantify the contributions of other processing variables relative to the potentials in controlling convection and segregation by reducing gravity. Given alternatives and a limited budget, any research is most likely to choose the less exotic ground-based research program.

2. Some significant numbers characterizing the capability of present HgCdTe production techniques are given below.

- Compositional uniformity, which determines the long wavelength cutoff, is claimed to be within 1 to 5 percent across a 1-cm wafer. (Device performance, characterized by D^*_λ may vary by about 50 percent.
- Excess carrier concentration at 77°K is within a compensated range of 1 to 2 x 10^{14} cm^{-3}. This extrinsic value may be due to defects or impurities.
- Carrier lifetimes are limited by extrinsic properties to about 1 μsec.

3. An assessment of NASA and DOD needs in the visible and infrared regimes lead to the comparison shown in Figure I-1 and the observations made below.

- NASA and DOD spectral needs overlap, but each agency has unique requirements.
- Earth-applications and planetary program thrusts are for fine spectral differentiation in the visible and color infrared regimes and in the thermal regimes.
- DOD thrusts are in the areas of surveillance and target signature.
- Space applications, NASA's prime mission, place difficult constraints on the use of Hg containing compounds because of the volatility.
- Ternary compounds could potentially satisfy all of NASA's requirements with more spectral flexibility and conversion efficiency than the present array of binary and doped elemental materials.
- It might be worthwhile for NASA to focus its efforts on the non-mercury (or non-volatile) compounds, which could be easier to produce and have longer space life.

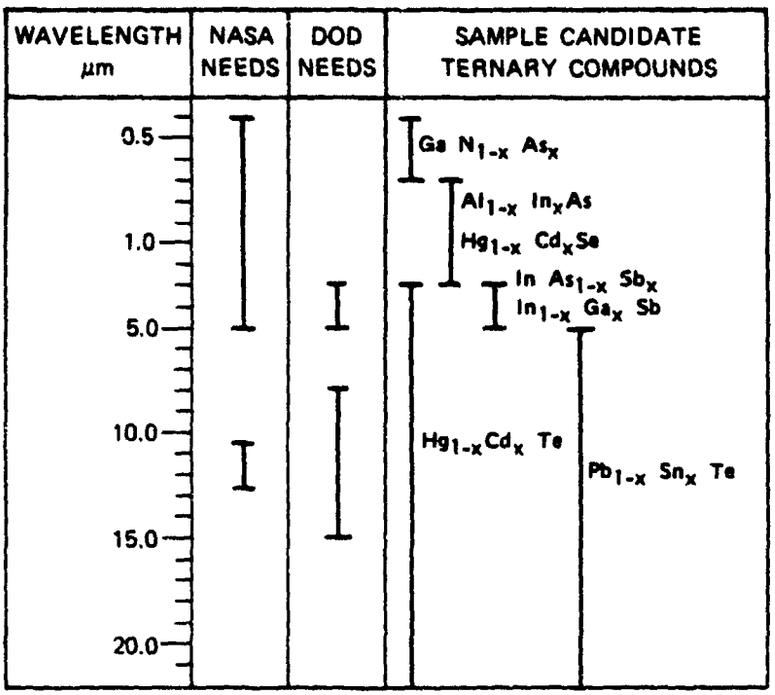

FIGURE I-1. TERNARY COMPOUND SELECTION

4. An assessment of ongoing ternary activities is examined in Table I-1 relative to the candidate ternary material options. The following statements highlight the key points in this area:

- Emphasis in DOD and NASA is on HgCdTe compounds.
- Both NASA and DOD could benefit by broadening the scope of their respective ternary compound option work beyond the few exploratory studies presently under way.
- Efforts on growth facility diagnostics generally appear to be lacking, though some of this is due to proprietary aspects. Relaxation of this problem would aid progress.
- NASA's defect/dopant chemistry work at Honeywell is particularly valuable and needs to be expanded to other materials.
- Some NASA or military laboratory needs to take the lead in evaluating diagnostic measurement capabilities and establishing standardized test methodologies.
- Lifetime studies need more emphasis.
- Ternary device production is perhaps focused on one of the more difficult material combinations to process and to prevent from decay.

TABLE I-1. RESEARCH FOCUS FOR CANDIDATE MATERIALS WITH SPECIFIC BANDWIDTH CAPABILITIES

Military Interest  NASA Interest 

			HgCdTe	PbSnTe	InAsSb or InGaSb	AlInAs or HgCdSe	GaNAs
			3-50 μm	5-50 μm	3-5 μm	0.7-3 μm	0.4-0.7 μm
Fundamental Properties	Phase diagrams, partial pressure	Stoichiometric	MACDAC (NASA) Marquette (AF)				
		Non stoichiometric					
		Impurity effects					
		Additive effects					
	Diffusivities, conductivities, ER	Stoichiometric					
	Band gaps and fermi energies	Stoichiometric					
		Additive effects					
Growth Techniques	Bridgeman (Contained melt)	Facility diagnostics	Clarkson (NASA)				
		Load assessments	NASA Inhouse				
			Honeywell (AF)				
			Hughes (AF)				
		Special problems	New England RC (AF)				
	Floating melt	Facility diagnostics					
		Load assessments					
		Special problems					
	Pull from crucible (Czochralski)	Facility diagnostics					
		Load assessments			Rockwell (NASA,AF)		
		Special problems					
	Rheocasting	Feasibility study	(ARPA)				
	Liquid Phase Epitaxy	Facility diagnostics					
		Load assessments	MIT (ARPA),TI(ARPA)				
			Honeywell (AF)				
			Hughes (AF)				
			Army Inhouse				
		Special programs	MIT (NASA)				
	Vapor Phase Epitaxy	Facility diagnostics					
		Load Assessments		MACDAC(NASA)			
		Special problems					
	Molecular Beam Epitaxy	Facility diagnostics	N. Carolina S. (AF)				
			Rockwell (ARPA)				
		Load assessments	Army Inhouse				
	Diode Sputtering	Feasibility study	New Jersey IT(AF)				

TABLE I-1. (CONTINUED)

Military Interest ▨ NASA Interest ▨

			HgCdTe	PbSnTe	InAsSb or InGaSb	AlInAs or HgCdSe	GaAlAs
			3-50 μm	5-50 μm	3-5 μm	0.7-3 μm	0.4-0.7 μm
Performance Assessment	Electrical Performance vs. Atomic Composition and Structure	Defect chemistry					
		Dopant Chemistry	Honeywell (NASA)				
		Laser Absorption	Colorado I.T.(AF)				
		Diagnostic Techniques	NASA Inhouse				
			New Jersey I.T.(AF)				
			U. Illinois (ARPA)				
Lifetime Decay	Electrical Performance	Surface Defect Migration	Army Inhouse				
	Decay with Time	Substrate Defect Migration					
		Volatile Constituent Loss	Army Inhouse				
		Magnetic field Enhancements	MACDAC(AF)				
Device Production	PV Detectors	Planetary Imagers		(NASA)			
		Common FLIR Module	Martin/Honeywell(A)	(NASA)			
			Texas I(A)				
			Hughes (A)				
		Thermal Sights	Hughes (A)				
			Honeywell (A)				
		Tank FLIR	Honeywell (A)				
		Fire & Forget	(A)				
		Optimization	Hughes(AF)		Rockwell (AF)		
		Hidas	Honeywell, (A, AF, M)				
		Communications	Hughes (AF)				
		Stare Mode	Honeywell (A,M)		Rockwell(A,M)		
			Texas Inst.		Hughes		
	MIS Detectors	Optimization	Texas Inst.(AF)				
		Hidas	Texas Inst. (A, AF, M)				
	Passivation	General Research	Army Inhouse				
		3 μm Instability	(AF)				
		Deposition Silicon Oxide	Hughes (AF)				
		Ion Implanting	Stanford (ARPA)				
		Passivant Characterization	Hughes (ARPA)				
			Stanford (ARPA)				
	Other	Beam Processing	New England (ARPA)				
		Hardening of Detectors	(A)				
		Gates on Epitaxial CCDS	(A)				

D. RECOMMENDATIONS

The following courses of action are recommended for consideration by the Materials Processing in Space Program. Initially we are suggesting some workshop-like meetings, first to review needs and assess directions, and then to delineate specific scientific focuses and the possibilities for joint or interrelated efforts between NASA and DOD.

1. An internal reevaluation needs to be made of the NASA visible and infrared sensor program, not in terms of the best way to implement an array sensor with maximum DOD inheritance, but rather in terms of the specific NASA detector needs and the specific matches with the spectral capability potentials of the full array of feasible ternary (and possibly quaternary) compounds. This would entail:

- Gathering appropriate representatives from the Headquarters Program Offices for Materials Processing (EM), Resource Applications (ER), Environmental Applications (EM), Planetary (SL), Astronomy (SA), and Sensor Research (RE) and from their mission and technology counterparts at MSFC, GSFC, LaRC, JPL, JSC, and NSTL/ERL.
- Exploring program needs for spectral range and narrowness of individual bandwidths, constraints in optics and detector-array packaging due to space implementation, and the material options for satisfying these needs.

2. An internal/external evaluation needs to be made of the priority directions for focus in visible and infrared detector research--from fundamental properties, to crystal growth dynamics, to the understanding of defect and additive chemistry, and to the interplay with other phases of the data processing chain through improved understanding of layering or other forms of attachment junctions. Three types of meetings, conducted in series, are recommended:

- The subset of NASA personnel involved specifically with the crystal growing and device junction problem in detector production needs to meet with selected university personnel (MIT, Marquette, Stanford, etc.) to evaluate biases and constraints in NASA interests and capabilities. From this background, they can then establish and identify specific research needs, establish scientifically defendable justification for program activity, and establish basic priorities for the application of funds.

- The second meeting in this external interface series would involve a subset of the NASA and university personnel (cannot be larger than the number of new participants) and a representative set of industry personnel from the seven or more industry organizations carrying out the major activity in detector science and commercial crystal growth. This would include two Honeywell organizations, two Hughes organizations, Texas Instruments, Rockwell, and McDonnell Douglas.[1] The purpose of this meeting is to establish, at least qualitatively, what has been done in each area, what feasibility questions have already been established but not reported, and where the greatest interest and capability exists for each task area. A priority adjustment is expected to take place after this meeting.
- The third meeting in this external interface series would involve the same subset of NASA and university people plus representatives from each of the major military visible-and-infrared sensor programs and device technology programs. In this meeting, the results of previous meetings would be presented, the opportunities for cooperative ventures discussed, and arrangements would be made for further meetings at individual locations to expose the ideas to a wider audience, to explore in more detail these or other joint opportunities, and to establish an initial basis for cooperative effort. Again we expect another adjustment in priorities from this third meeting and the additional meetings it generates.

3. There are a number of areas which we recommend for particular consideration. These are summarized below and discussed further in Section V.

- All of the possible ternary (and some of the quaternary) options need to be systematically assessed as to their potential for continuous control (through composition variation) of the effective cutoff wavelength. Particular attention should be given to volatility of constituents in the space environment and any peculiarities of chemistry that might portend decay in aircraft or other earth environments.
- Phase diagrams should be generated for all of the material combinations that appear promising from either a performance or lifetime point of view.
- Diagnosis of the actual thermal geometries of each of the major crystal growing configurations is a basic datum that needs to be established before much sense can be made out of variations in the material input loads in terms of stoichiometry, graded compositions in starting volumes, impurity and additive variations, etc. These diagnostic data are generally not available, either through

[1] The activity represented by Reference 5 involves these people, but addresses the wrong issues.

neglect or lack of reporting. Although it needs to be assessed in more detail, our assessment implies that NASA should take the lead in the bulk techniques and in vapor phase epitaxy. The military might take the lead in liquid phase epitaxy and molecular beam epitaxy. Both should look at remelt techniques with high-intensity local heating.

- Defect and dopant chemistry efforts need to be expanded to a wider variety of ternary materials based on the more general material assessment and phase diagram results. Stoichiometric and nonstoichiometric mixtures, variations in impurities and contaminant levels, variations in dopant and compensator levels, growth technique contributions, and annealing effects all need close study. Military emphasis should be on HgCdTe materials while NASA could pick up on some of the other ternary options.
- Special studies on Marangoni effects, flat-sided ampules, multilayering techniques, hardening, etc., should continue as appropriate interest is matched with available capability.
- Diagnostic instrumentation needs t be evaluated as to its contribution to knowledge about electrical, compositional, and structural properties of crystals. Special attention should be given to the potential for standardized diagnostic techniques and to assigning priorities for development of each of the techniques. A NASA or military laboratory should take the lead in this effort or work interactively with an NBS lead in this effort.
- Junction research needs to be evaluated relative to the variation in problems with the array of ternary options available. Would ease of attachment drive selection towards specific ternaries? Or is the problem of a more general nature, with HgCdTe a representative example? We did not explore this area in enough depth under this contract to make specific recommendations.
- Device production needs to be considered as a major factor in material and growth-technique selection. All of the steps in device production contribute to performance and lifetime. More effort would be needed to make a consistent set of recommendations in this area.
- Space-based crystal growth of ternary and quaternary compounds becomes important in the material combinations with wider variations in the relative densities of their binary constituents. Several of the candidate materials suggested earlier may indeed be easier to grow under low gravity conditions. More information is needed to confirm this supposition.

- Lastly, our interfaces with university and industry personnel as well as military personnel lead us to believe that NASA could benefit from improved communication with these people through a newsletter, through greater open literature publication, through greater meeting attendance, and through systematic visitations with key researchers. NASA, in this program, still gives off the aura of an exotic flower with its roots in the trees rather than on the ground.

II. FOCUS OF IR TECHNOLOGY

A. IR DETECTOR TECHNOLOGY

In the recent past there has been a mixed approach to IR detector development. Research has been driven by the desire for multielement focal plane arrays with onboard processing capability. For a while, extrinsic silicon received considerable attention because of the mature technology evolved for fabricating silicon electronic structures. However, any extrinsic device suffers from inherent problems of low operating temperatures, which are needed to freeze out charge carriers contributed by unwanted shallow impurities, and low quantum efficiencies due to finite solubilities of dopants. An extrinsic detector, being a photoconductive device, also requires a bias current of significant magnitude, which results in undesirable power consumption and joule heating. Furthermore, the efficiency of an extrinsic detector requires additional thickness, leading to optical crosstalk in dense arrays. All of these faults inhibit the development of cheap, compact, and reliable imaging detectors. On the other hand, an intrinsic detector provides a larger quantum efficiency and can be manufactured in a high impedance photovoltaic structure. Unfortunately, the desired spectral bands are not covered by the available elemental and compound semiconductors. The most promising materials, with respect to detector properties, are the alloy solid solution semiconductors in which the spectral response is determined by the relative proportion of the constituents. Of the two major contenders, PbSnTe and HgCdTe, HgCdTe, which can span the largest spectral band of interest, has recently been found to offer the greatest potential as an IR detector material. The short-term prospects seem to favor a hybrid design in which a HgCdTe detector array is coupled to a silicon or HgCdTe CTD array for readout and processing. If the technology matures in building electronic structures

from HgCdTe substrate with the same ease as it did with silicon, one can expect monolithic arrays. This will, however, depend on the ability to prevent detector element degradation during the numerous processing steps required to build the CCD and related structure.

Since the demand for HgCdTe is miniscule compared to that for silicon, research in the processing of single crystal material has not been great. The greatest expertise has resulted with only a few people in a handful of organizations, both Government and commercial. Since the material is a high-cost item, the significant details of processing are well guarded trade secrets. In addition, many of the device performance requirements are not available because of security classification. Discussions with various individuals who are involved in the field indicate that there are significant differences as to the capabilities and limitations of the material currently available. A summary of the information obtained from these discussions follows.

1. Compositional Uniformity

The proportionality factor x in $Hg_{1-x}Cd_xTe$ determines the wavelength at which the detector's peak spectral response occurs. There is a desire for large wafers of 2 to 3 inches in diameter for which the composition varies by less than 1 percent. Honeywell currently claims to produce bulk single crystals 1/2 inch in diameter and 4 inches in length for which 95 percent of the material has less than a 1-percent variation. They expect to be producing 1-inch-diameter crystals shortly and 3-inch-diameter crystals later on. Other sources indicate that the uniformity of available material is not this good (5 percent or more).

2. Carrier Concentration

Detector performance is maximized by minimizing the density of thermally induced carriers. The ideal situation occurs for perfect intrinsic material. Table II-1 indicates the intrinsic density of electrons and holes for various cutoff wavelengths and temperatures in HgCdTe. These density values are increased by the presence of impurities or stoichiometric defects which make the material either n or p type. Honeywell indicates

TABLE II-1. INTRINSIC CARRIER CONCENTRATION IN HgCdTe FOR REPRESENTATIVE VALUES OF CUTOFF WAVELENGTH λ_{co} AND OPERATING TEMPERATURE T[a]

		λ_{co} (μm)				
n_i (cm^{-3})		3	5	8	10	12
T (°K)	77	5.7×10^{3}	9×10^{8}	6.6×10^{11}	5.7×10^{12}	2.3×10^{13}
	190	2×10^{12}	2×10^{14}	2.5×10^{15}	5.4×10^{15}	8.9×10^{15}
	300	4×10^{14}	6.7×10^{15}	2.7×10^{16}	4.2×10^{16}	5.5×10^{16}

[a]See equation below:

$$n_i \ (cm^{-3}) = 5\times10^{14}\ \lambda_{co}^{-3/4}\ (\mu m)\ T^{3/2}\ (°K)\ \exp\left(-\frac{1.23}{2\ kT\ \lambda_{co}}\right)$$

chemical impurities present at about 10^{14} cm^{-3}. These impurities are not frozen out at low temperatures (~4°K). Others attribute the carriers to deviations from stoichiometry. High concentrations of carriers are typically reduced by compensation with shallow impurities or defects of the opposite type. The operating range of carrier concentration in Honeywell detectors is $1\text{-}2\times10^{14}$ cm^{-3} at λ_{co} = 10-12 μm and 77°K. The compensation reduces the carrier concentration but may also affect carrier lifetime and mobility in an adverse way.

3. Carrier Lifetime

For high-sensitivity devices, it is necessary that recombination does not occur until a significant portion of the photon-induced charges are collected. Current values of carrier lifetime are about 1 μs, with a need for about 5 μs. Recombination may occur by one of three basic mechanisms: Shockley-Read recombination, Auger recombination, or radiative recombination. Shockley-Read recombination involves an intermediate transition to an intergap energy level provided by an impurity or defect which attracts both

an electron and a hole. The lifetime is inversely related to the number of such levels and to their position in the energy gap. This mechanism is dominant in materials with considerable impurities, in p-type material, and at very low temperatures. Auger recombination involves the interaction of a third carrier (usually an electron) with the recombining electron-hole pair to absorb the energy and jump to a higher level in the conduction band continuum. This is followed by an immediate cascade to a lower level with the creation of lattice energy (phonons). The lifetime for this process is inversely related to the product of n^2p, where n is the electron concentration and p the hole concentration. This mechanism is dominant in n-type material. Radiative recombination involves the direct recombination of an electron-hole pair with the emission of a photon. This mechanism gives a lifetime inversely related to the np product and dominates in nearly intrinsic material at very low temperatures.

4. Carrier Mobility

At high temperatures, the mobility of the carriers is limited by lattice scattering (phonon interactions). At lower temperatures, mobility is diminished by the presence of ionized impurities. In photoconductors, a high mobility ratio of electrons to holes is desired for high gain with a low overall mobility to prevent impact ionization.

5. Frequency Response

A wide frequency bandwidth is desirable for detectors using laser heterodyning and for optical communications. A bandwidth of 2 GHz has been achieved and a desired goal is about 5 GHz. Large bandwidths require short carrier lifetimes, and detectors must be designed to have low capacitance values to minimize the RC time constant of the circuit. The present limitation to 2 GHz is not fully understood.

6. Dislocation Density

People typically express a desire to lower the dislocation density. However, with operating devices having minor type dislocation densities ranging from 10^3 to 10^7 cm^{-2}, there seems to be no clear correlation pointing to this as a source of degradation in device performance.

7. Quench/Anneal Processing

Honeywell has had success with growing large HgCdTe crystals (1/2 x 4 inches) by a quench/anneal process. The quenching part provides an overall macroscopic compositional uniformity. The high-temperature anneal promotes the growth of a single crystal. In this process, CdTe microprecipitates and Hg occlusions are swept out. Material with lower values of x (long wavelength cutoff) are easier to produce because of the faster diffusion of Hg. Stoichiometry is adjusted in wafers by controlling the mercury vapor pressure during the annealing process. The entire process takes 6 to 10 weeks.

8. Liquid Phase Epitaxy

Researchers at Honeywell, Rockwell, and Lincoln Labs have indicated success with horizontal LPE on CdTe or CdTeSe substrates from a tellurium-rich solution. This method, using an open tube slider approach, produces a uniformly thick layer with compositional variations kept to within a few percent over areas on the order of 1 cm^2. This method may be used to produce multi-layer structures.

9. Prognosis

There are really two divergent opinions concerning the present state of the art. Suppliers of devices are generally optimistic and do not admit any insurmountable problems in achieving theoretically limited performance. They typically believe that further refinements of their apparatus can increase the yield of high-quality devices. Users, on the other hand, are not satisfied with the nonuniform responses present in the small arrays (typically 32 x 32 elements) currently available and are skeptical about achieving desirable results for larger (1,000 x 1,000 elements) arrays. The present detector arrays in operation are usually photoconductive (PC) and employ either software or hardware to compensate for irregularities. A frequently used technique is that of time delay and integration (TDI),

which mechanically scans an image over several array elements and averages the signal output. The large arrays of the future will need to operate in a staring mode with a one-to-one correspondence between source and image. The presence of hardware circuitry for image enhancement would be unmanageable for million element arrays, as would be computer software compensation.

At least for the smaller arrays, the large variations of response (as much as 50 percent) are less due to gross compositional differences (kept to about 1 percent) than to microscopic variations of defects and/or impurities. These extrinsic factors give rise to a higher noise level from increased ambient carrier concentration and decreased carrier lifetime. It is extremely important to isolate and eliminate these extrinsic factors. Presently, it is not established whether or not some of these degrading elements are introduced in the bulk processing of the material or in the device fabrication.

B. PRESENTATION FORMAT

In conducting this study on the utility of space processing experiments in the production of high-quality infrared detector crystals, it was recognized at the start that any successful program of soliciting the participation of agencies outside of NASA would depend on the judgments of three types of people. One, the scientist would have to recognize a physical rationale for expecting the space environment to provide tangible benefits. Two, the engineer would have to be convinced that equipment could be fabricated to properly exploit the advantages of the space environment without yielding to any disadvantages. Three, the program manager must have sufficient information to evaluate the risks and benefits in terms of the time and money spent on a space processing venture as opposed to other more conventional programs. A successful presentation must therefore be directed towards representatives of all three classes. A major problem is to devise a presentation that would, in a short time, simultaneously stimulate the interest of members of these three groups. The prime target in the audience is, of course, that individual who controls the direction and/or funding of research efforts.

The formal presentation should be kept to a relatively simple level to be understandable to all three groups. Any technical discussion should be in response to questions from the audience. In some instances, it may be expected that members of any one of the three groups may have only a limited knowledge of the other groups' fields. A discussion of the fundamentals of both the detector and materials processing physics would be suitable.

Chapter III presents a fairly thorough treatment of the theory of IR detection and points out those aspects of a material that will enhance or degrade detector performance. Chapter IV is a less detailed overview of the subject of crystal growth. It is meant to provide a framework for a presentation to an audience that is not well versed in that subject. Both of these chapters, along with providing guidance for any presentation, may also be distributed as informational material. A list of the pertinent publications consulted in generating Chapters III and IV is provided at the end of the report. Chapter V evaluates the present NASA and military programs in IR detector materials and makes recommendations for NASA consideration.

III. DETECTOR MATERIALS SCIENCE

A. INTRODUCTION

The goals of this chapter are:

- Provide a common base of information on detector materials science that can be communicated efficiently to a diverse audience containing program managers, application engineers, and materials scientists.
- Prepare a framework for integration of data on many different materials and physical processes.

In order to attain these goals, the following three basic questions are addressed:

- What materials are useful for infrared detectors?
- How can one gauge the difference between actual and potential detector performance?
- How does material structure affect detector performance?

B. DETECTOR

Since the semiconductor's electronic bandgap determines the minimum photon energy or maximum wavelength to which the detector is sensitive, various materials provide detection capabilities in different portions of the infrared spectrum. Furthermore, the detection response is not the same for all radiation of a wavelength less than the maximum; the response generally increases with increasing wavelength and peaks at a wavelength slightly shorter than the maximum.

In order to minimize attenuation due to atmospheric absorption and scattering, detectors are often designed to operate in the middle infrared region between 3 and 5 μm or in the thermal infrared between 8 and 14 μm. These windows are not completely transparent: there is, for example, a major decrease in transmittance at 9.5 μm due to ozone.

It is thus of interest to correlate the maximum detectable wavelength of various materials with the usable regions of the infrared spectrum. Figure III-1 displays this information for several elemental, doped elemental, binary, and ternary semiconductors.

We see that the 3- to 5-μm region is accessible to silicon doped with selenium (Group VI) or thallium (Group III), to the IV-VI compounds PbS, PbSe, and PbTe, and to the III-V compound InAs. It is also accessible to the II-VI ternary alloy $Hg_{1-x}Cd_xTe$ if x has a value between 0.3 and 0.4.

The 8- to 14-μm window allows fewer possibilities: silicon doped with magnesium, $Hg_{1-x}Cd_xTe$, or the IV-VI ternary allows $Pb_{1-x}Sn_xTe$. For either of the ternary alloys, the required value of x is approximately 0.2.

Another salient feature of Figure III-1 is the dependence of the maximum detectable wavelength upon the composition of the ternary alloys. As the compositional variable, x, is varied from zero to 1, the maximum wavelength changes from the value associated with one pair of the three elements (e.g., HgTe) to that associated with the other pair (e.g., CdTe). This situation may be contrasted with the behavior of the doped and binary semiconductors, the maximum wavelength of which is fixed by the elements involved.

Empirical equations that relate the maximum detectable wavelength to the compositional variable are available; for $Pb_{1-x}Sn_xTe$,

$$\lambda_{co}(77°K) = (0.175-0.406x)^{-1} \ \mu m$$

while, for $Hg_{1-x}Cd_xTe$,

$$\lambda_{co}(T) = [1.28x + 0.264x^3 - 0.20 + 4.22 \times 10^{-4}(T)(1 - 2.08x)] \ \mu m.$$

Figures III-2 and III-3 display these relationships.

If we desire uniformity in the cutoff wavelength of various samples of $Pb_{1-x}Sn_xTe$, we see that much less precision in the x-value is required when

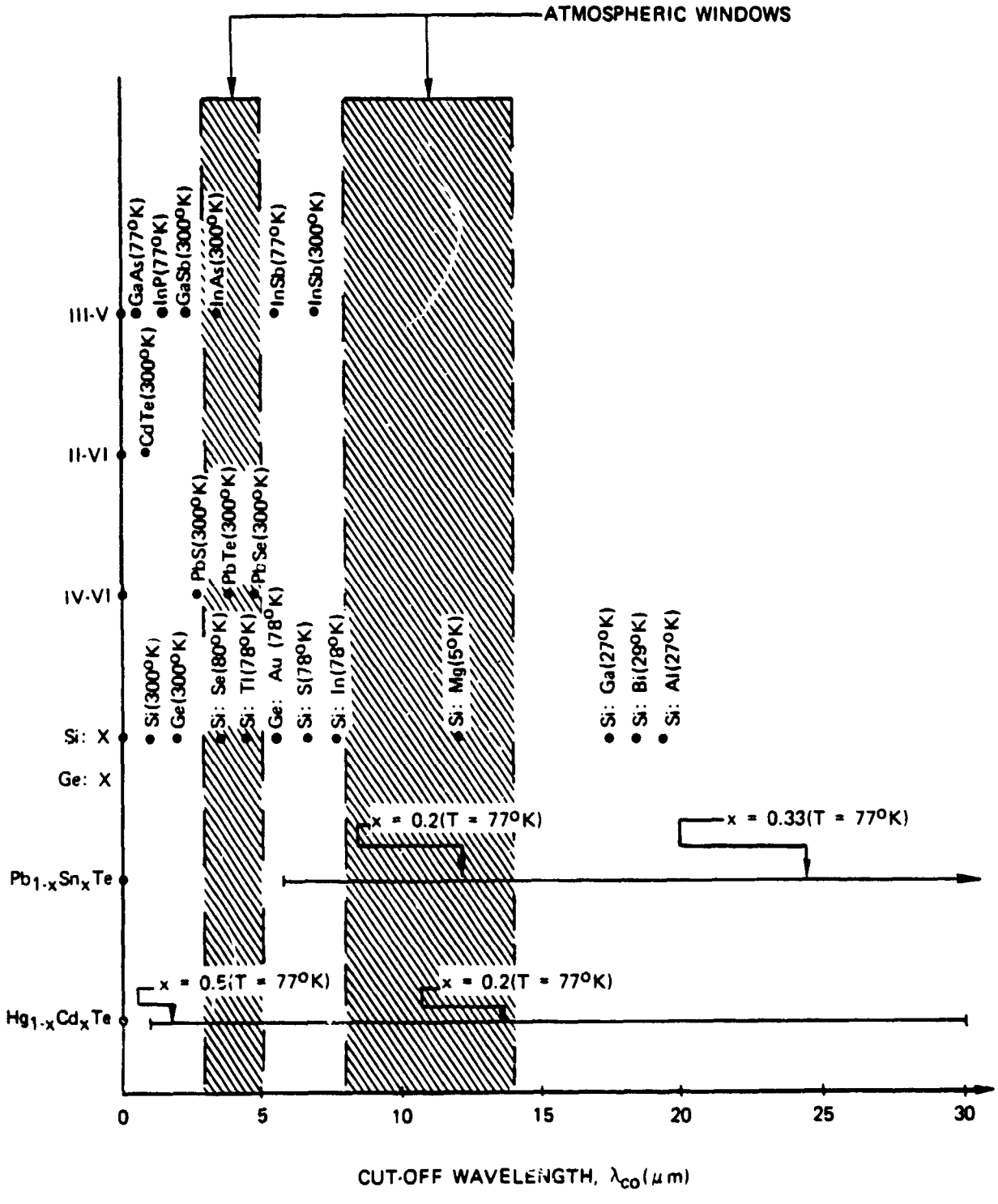

FIGURE III-1. CUT-OFF WAVELENGTHS OF INFRARED DETECTOR MATERIALS

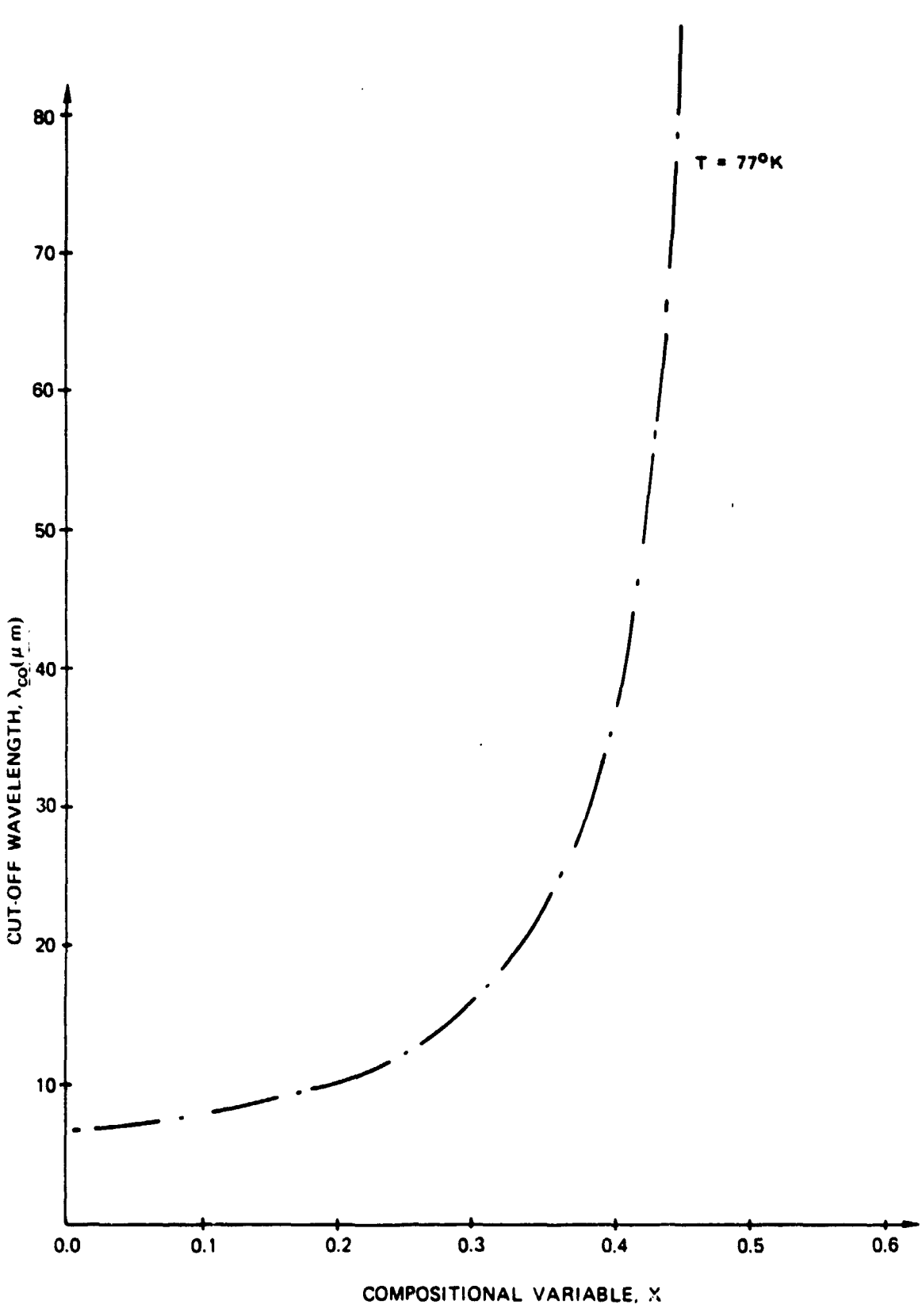

FIGURE III-2. CUT-OFF WAVELENGTH AS A FUNCTION OF COMPOSITION FOR $Pb_{1-x}Sn_xTe$

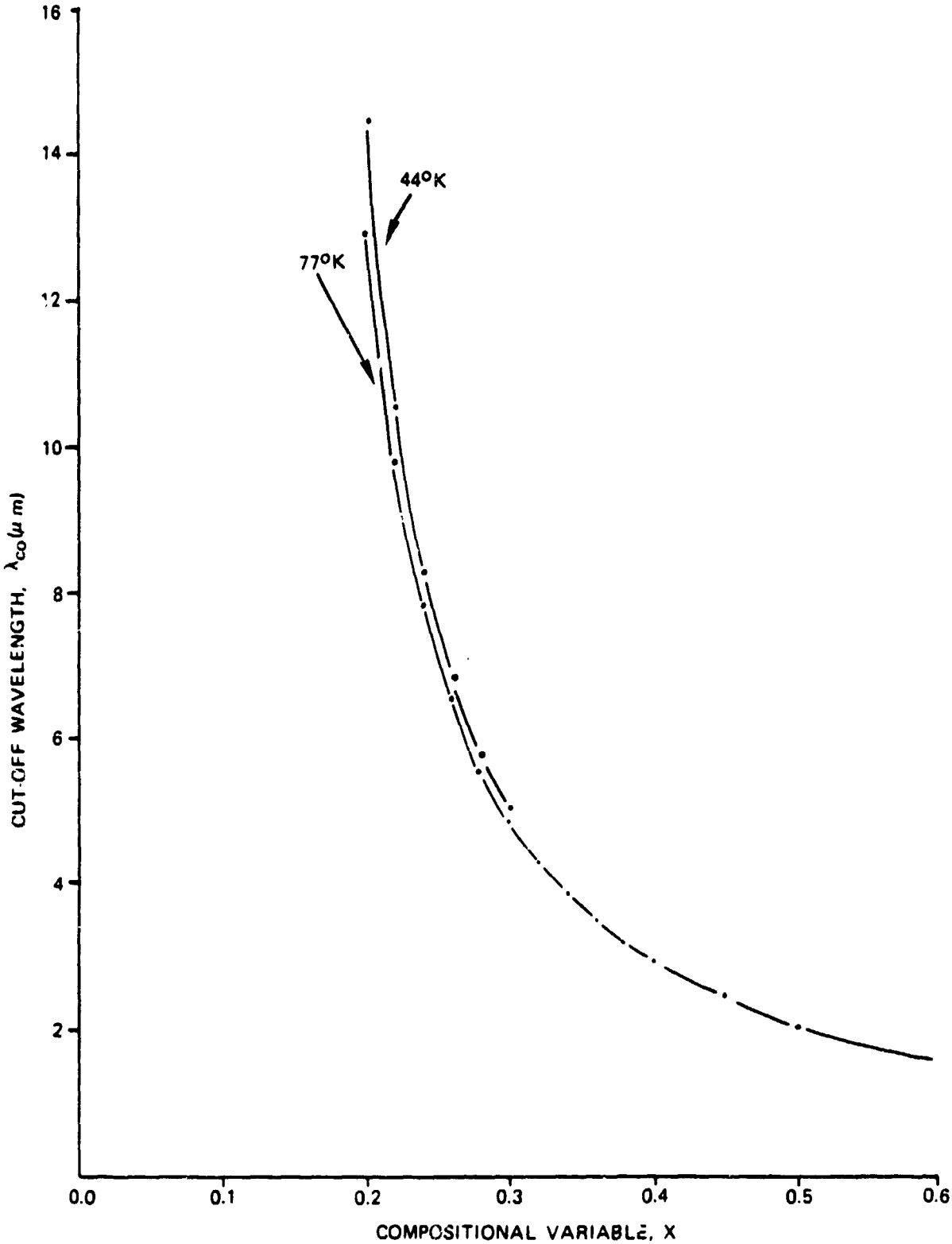

FIGURE III-3. CUT-OFF WAVELENGTH AS A FUNCTION OF COMPOSITION FOR $Hg_{1-x}Cd_xTe$

λ_{co} is less than 18 μm. If λ_{co} must lie between 10 and 11 μm, x may vary by about 10 percent from 0.19 to 0.21. However, if λ_{co} must lie between 30 and 31 μm, then x may vary only by about 1 percent from 0.349 to 0.352.

Similar uniformity in $Hg_{1-x}Cd_xTe$ requires less precision in the x-value when λ_{co} is less than 5 μm. At an operating temperature of 77°K, if λ_{co} must lie between 3 and 4 μm, then x may vary by about 17 percent from 0.397 to 0.335. However, if λ_{co} must lie between 10 and 11 μm, then x may vary only by about 3 percent from 0.217 to 0.211.

C. MODES OF DEVICE OPERATION

There are two principal ways to utilize semiconductors as photon detectors in the infrared portion of the spectrum. In the first, the material serves as a photoconductor; in the second, it serves as a photodiode.

The phenomenon of photoconductivity is based on the internal photoelectric effect: light quanta excite charge carriers inside the material, thus altering the material's electrical properties. Pure semiconductors are known as intrinsic photoconductors, since quanta excite electrons across the bandgap from the valence band to the conduction band. Doped semiconductors are known as extrinsic photoconductors since energy levels created by an impurity inside the bandgap are involved in acceptance of an electron from the valence band or donation of an electron to the conduction band.

In either photoconductive case, the method of photon detection is to monitor the change in conductance of the semiconductor when it absorbs radiation. Figure III-4 gives a schematic circuit diagram for the photoconductive mode. If R_L is the load resistance, R_D the dark or uniliuminated resistance of the photoconductor, and V_0 the applied voltage, then the load voltage is given by

$$V_L = \frac{V_0 R_L}{R_D + R_L} .$$

We monitor changes in R_D by observing changes in V_L, since, for small changes

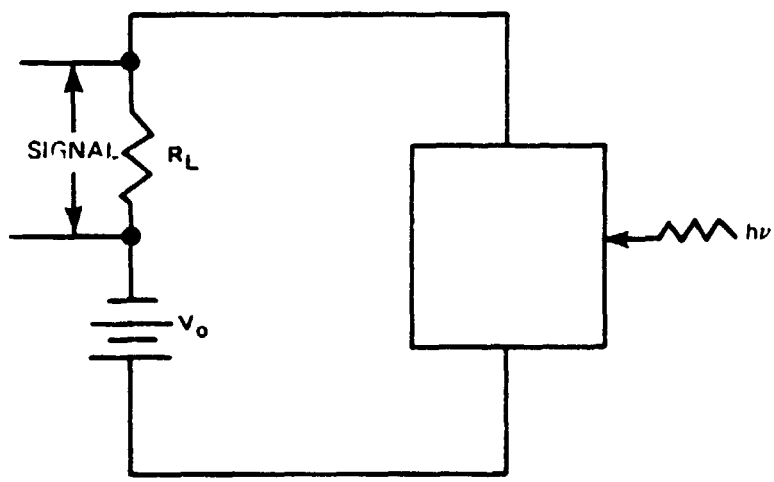

FIGURE III-4. SCHEMATIC CIRCUIT DIAGRAM FOR PHOTOCONDUCTORS

$$dV_L = - \frac{V_0 R_L}{(R_D+R_L)^2} \, dR_D \quad .$$

The simplest semiconductor photodiode is constructed from two types of material: one rich in electrons (n-type) and one rich in holes (p-type). Juxtaposition of these two types creates a junction region in which there is a strong electric field pointing from the n-type to the p-type material. When radiation is absorbed in the junction region, electrons may be excited into the conduction band from the valence band; the local electric field will separate the electron-hole pair thus created and give rise to a measurable current. Monitoring this current allows one to detect radiation. Figure III-5 gives a schematic diagram of a p-n semiconductor photodiode.

The interfacial zone in a junction photodiode is often labelled the depletion layer since the density of free charge carriers is very low in this region. The width of this region can be controlled by the voltage applied across the photodiode. If the p-type side is maintained at a higher potential than the n-type side, the device is said to be reverse-biased and the width of the depletion layer is increased. This means that more electrons excited by incident radiation will be close to the junction region; this will increase the photocurrent and improve sensitivity. Increasing the width of the depletion layer reduces its capacitance; this decreases the RC time constant of the photodiode circuit and therefore lowers its response time.

One may increase the width of the depletion layer still further by separating the p-region from the n-region with a layer of intrinsic material. This relatively wide, undoped layer increases the sensitivity and decreases the response time under reverse-bias conditions. This structure is known as a p-i-n photodiode.

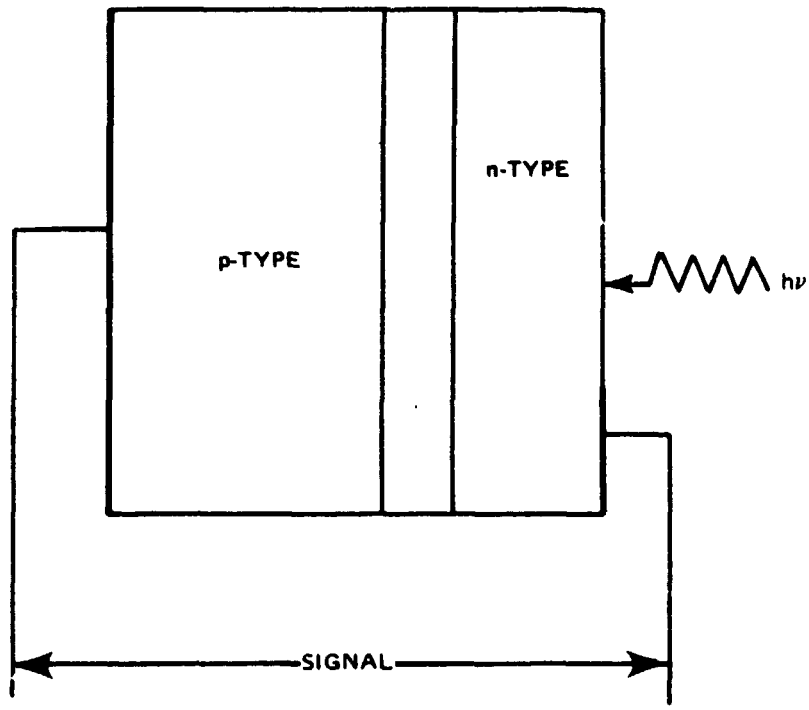

FIGURE III-5. SCHEMATIC CIRCUIT DIAGRAM FOR UNBIASED P-N PHOTODIODES

D. GENERATION OF NOISE

A semiconductor-based detector is subject to several types of internal noise-generating processes. The most prevalent of these is caused by the random, thermal motion of charge carriers and is known as thermal, Johnson, or Nyquist noise. Its magnitude depends upon the temperature (T), the detector bandwidth (B), and the detector resistance (R):

$$V_{thermal}^{rms} = \sqrt{4kTRB} \quad .$$

A second type of internal noise is known as 1/f noise since its power is inversely proportional to the frequency. This noise is also called flicker noise. The physical process that produces this noise is not clearly understood, though it may be related to interfacial phenomena.

A third sort of internal noise is caused by fluctuations in the concentration of charge carriers in the semiconductor due to thermal variations in the rates of carrier generation and recombination. When current flows through the device, this concentration change appears as an alteration of the device resistance. Expressions for the voltage due to this generation-recombination (g-r) noise are highly dependent upon the nature of the semiconductor. For an extrinsic material with a single impurity level used as a photoconductor at low temperature, the voltage is

$$V_{g-r}^{rms} = 2I_b R \left[\frac{\tau B}{N\,(1+\omega^2\tau^2)}\right]^{1/2} \quad ,$$

where I_b is the bias current, N is the number of free carriers in the material sample, and ω is the frequency divided by 2π. In an intrinsic photoconductor, the number of free electrons (N), the number of free holes (P), and the ratio of electron mobility to hole mobility (b) enter the expression as follows:

$$V_{g-r}^{rms} = 2I_b R \left(\frac{b+1}{bN+P}\right)\left[\frac{NP}{N+P}\left(\frac{\tau B}{1+\omega^2\tau^2}\right)\right]^{1/2} \quad .$$

E. CARRIER LIFETIME

A charge carrier adds to the photocurrent only so long as it exists in a conductive band. This state may be curtailed by any of a number of processes, the strength of which depends on the characteristics of the material. Assuming homogeneous material for which the competing processes of generation and recombination are occurring uniformly, one can designate a characteristic lifetime for a density of N_e excess electrons as

$$\tau = \frac{N_e}{r-g}$$

where r and g are the rates of recombination and generation. When a number of such r and g processes exist, the lifetime is given by

$$\frac{1}{\tau} = \sum_i \frac{1}{\tau_i} = \frac{1}{N_e} \sum_i \frac{1}{r_i - g_i} \quad .$$

Three major mechanisms limit the lifetime of a free carrier:

- Radiative recombination: The free carrier loses energy by photon emission.
- Auger recombination: The free carrier loses energy to another carrier.
- Shockley-Read recombination: The free carrier loses energy and is trapped at an interband level caused by an impurity or lattice flaw where it may then recombine with a complementary carrier.

1. Radiative Recombination

Intrinsic Material. At thermal equilibrium in the absence of external radiation, the rates of generation and recombination are equal and designated G_R. The value of G_R is a function of temperature and of the interactions which produce electron-hole pairs. At thermal equilibrium, the number of free electrons and free holes are represented by N_o and P_o with $N_o P_o = N_i^2$. The value of N_i, the intrinsic carrier concentration, is a function of band-gap, band shape and temperature. The recombination rate is intuitively proportional to the number of both negative and positive carriers.

This leads to

$$r_R - g_R = G_R\left(\frac{NP-N_i^2}{N_i^2}\right) .$$

The lifetime for any excess carrier N_e is

$$\tau_R = \frac{N_e}{r_R-g_R} = \frac{N_i^2}{G_R(N_o+P_o+N_e)} .$$

This function is a maximum for intrinsic material where $N_o = P_o = N_i$. For low flux rates, $N_e << N_i$ and

$$\tau_{R,\,max} = \frac{N_i}{2\,G_R} .$$

Extrinsic Material (Heavily Doped). In an n-type extrinsic material, N_d donors are added to such an extent that any low-lying acceptor levels N_a and the valence band are essentially full. The incident radiation will produce transitions from un-ionized donor levels to the conduction band. In the absence of external radiation at low temperature, the number of conduction electrons is N_o while the number of ionized donor states with which recombination can occur is $N_a + N_o$. The number of un-ionized donor states which can generate electrons is $N_d - N_a - N_o$. At equilibrium, the generation-recombination process has a rate G_R. When radiation is incident, we have

$$r_R = G_R\left[\frac{(N_o + N_e)(N_o + N_e + N_a)}{N_o(N_o+N_a)}\right]$$

$$g_R = G_R\left[\frac{(N_d - N_a - N_o - N_e)}{(N_d - N_a - N_o)}\right] .$$

The inverse lifetime for the decay of excess charges is then

$$\frac{1}{\tau_R} = \frac{r_R - g_R}{N_e} = \frac{G_R}{N_o}\left[\frac{(N_d - N_a)}{(N_d - N_a - N_o)} + \frac{N_o + N_e}{(N_o + N_a)}\right] .$$

A similar relation holds for p-type material when we substitute P_o, P_e, and N_a for N_o, N_e, and N_d.

2. Auger Recombination (Band to Band)

Intrinsic Material. In this process a free carrier recombines with the interband energy being transferred to another free carrier. This is much more significant in electron-electron interactions than in hole-hole interactions. The recombination rate involves a three-body process (two free electrons, one free hole) while the generative process (impact ionization) is only proportional to the number of free electrons. Therefore,

$$r_{ee} - g_{ee} = G_{ee}\left[\frac{N^2 P}{N_o^2 P_o} - \frac{N}{N_o}\right] ,$$

where G_{ee} is the interaction rate at thermal equilibrium. Thus, in the absence of hole-hole processes, the Auger lifetime is given by

$$\tau_A = \frac{N_e}{r_{ee} - g_{ee}} = \frac{N_i^4/G_{ee}}{(N_o + P_o + N_e)(N_o + N_e) P_o} .$$

Extrinsic Material (Heavily Doped). The recombination rate for material is

$$r_A = G_A\left[\frac{(N_o + N_e)^2 (N_o + N_e + N_a)}{N_o^2 (N_o + N_a)}\right]$$

while the generation rate is

$$g_A = G_A \left[\frac{(N_o + N_e)(N_d - N_a - N_o - N_e)}{N_o (N_d - N_a - N_o)} \right] .$$

The inverse lifetime is

$$\frac{1}{\tau_A} = \frac{r_A - g_A}{N_e} = G_A \frac{(N_o + N_e)}{N_o^2} \left[\frac{N_d - N_a}{N_d - N_a - N_o} + \frac{N_o + N_e}{N_o + N_a} \right] .$$

3. Shockley-Read Recombination

Between the conduction and valence bands, impurities and dislocations may create isolated energy states called traps. These traps may lead to recombination in a two-step process or they may release the captured carriers before recombination can occur. For a low density of traps, the lifetime is

$$\tau_{s-r} = \tau_{n_o} \left[\frac{(P_o + P_t + N_e)}{(N_o + P_o + N_e)} \right] + \tau_{p_o} \left[\frac{(N_o + N_t + N_e)}{(N_o + P_o + N_e)} \right] ,$$

where $P_t = P_o \exp \frac{\phi - E_t}{kT}$

$N_t = N_o \exp \frac{E_t - \phi}{kT}$

E_t = trapping level

ϕ = Fermi level

τ_{n_o} = electron trapping time by a neutral trap

τ_{p_o} = hole trapping time by a full trap.

F. OPTIMAL PERFORMANCE OF INFRARED DETECTORS

A common descriptor of detector performance is the spectral detectivity, D^*_λ, which varies directly with the signal current and inversely with the normalized noise current and the power of the incident photon flux. That is,

$$D^*_\lambda = \frac{I_s}{I_n P_\lambda} \quad .$$

The signal current may be written as

$$I_s = \frac{q\eta G\lambda P_\lambda}{hc} \quad ,$$

while the normalized noise current may be written as

$$I_n = \frac{i_n}{(A\Delta f)^{\frac{1}{2}}}$$
$$= Gqu^{\frac{1}{2}} \left(\eta\Phi_b + \frac{I_d}{qG^2A} + \frac{kT}{q^2G^2AR} \right)^{1/2}$$

where G = photogain, that is, the number of electrons flowing in the circuit per photon absorbed ($G = 1$ for simple photovoltaic detectors; $G \neq 1$ for photoconductive detectors)

q = charge on an electron

u = numerical factor ($u = 2$ for photovoltaic detectors; $u = 4$ for photoconductive detectors)

η = quantum efficiency

Φ_b = background photon-flux density

I_d = voltage-dependent dark current

A = detector area

R = detector resistance.

Hence, the detectivity becomes

$$D^*_\lambda = \frac{\eta\lambda}{hcu^{\frac{1}{2}}} \left(\eta\Phi_b + \frac{I_d}{qG^2A} + \frac{kT}{q^2G^2AR} \right)^{-1/2}$$

Maximal values of D^*_λ will be obtained when the expression in parentheses approaches a minimum value of $\eta\Phi_b$. This occurs when

$$\frac{I_d}{qG^2A} << \eta\Phi_b \qquad \text{[first inequality]}$$

and

$$\frac{kT}{q^2G^2AR} << \eta\Phi_b. \qquad \text{[second inequality]}$$

When these inequalities hold, the detectivity has attained its maximal background-limited value:

$$D^*_\lambda \text{ (BLIP)} = \max (D^*_\lambda)$$

$$= \frac{\eta^{\frac{1}{2}}\lambda}{hc\,(u\Phi_b)^{\frac{1}{2}}} .$$

Since the left sides of the inequalities can be related to material properties, we can usefully explore the conditions under which they will hold for various classes of detector materials. We shall discuss three types: intrinsic photoconductive detectors, extrinsic photoconductive detectors, and photovoltaic detectors.

1. Intrinsic Photoconductive Detectors

First, we will consider the intrinsic photoconductive detector. The material's bandgap energy, E, determines the maximum wavelength λ_c that the detector can absorb:

$$\lambda_c = \frac{hc}{E} .$$

It can be shown [Ref. 1] that the first inequality becomes

$$t\left(\frac{n_o}{2\tau_{Ai}} + R_r\right) << n\Phi_b$$

on the assumption that

$$\Delta n = \Delta p << n_o ,$$

where t = thickness of detector element
n_o = equilibrium concentration of electrons
τ_{Ai} = intrinsic Auger recombination lifetime
R_r = direct radiative recombination rate
Δn = photoexcited electron concentration
Δp = photoexcited hole concentration.

Since $R_r \alpha \exp(-E/kT)$ and $\tau_{Ai} \alpha \exp(E/kT)$, both R_r and $1/\tau_{Ai}$ grow as the temperature increases and the first inequality therefore places an upper limit on the operating temperature of the detector.

If we again assume that

$$\Delta n = \Delta p << n_o ,$$

then the second inequality,

$$G^2AR >> \frac{kT}{q^2 n\Phi_b} ,$$

becomes

$$\frac{[w(b+1)Z_h f(Z_h)]^2}{qt(nb+p)\mu_h} >> \frac{kT}{q^2 n\Phi_h}$$

for n-type intrinsic photoconductors and

$$\frac{[w(1+1/b)Z_e f(Z_e)]^2}{qt(nb+p)\mu_e} >> q^2 n\Phi_b$$

for p-type intrinsic photoconductors.

Note that $Z_h = \mu_h \tau_h E_{e/w}$

$Z_e = \mu_e \tau_e E_{e/w}$

$f(Z) = 1-Z\ [1-\exp\ (-\frac{1}{Z})]$

w = length or width of square detector element

$b = \mu_e/\mu_h$

μ_e = electron mobility

μ_h = hole mobility

τ_e = electron lifetime

τ_h = hole lifetime

n = electron concentration

p = hole concentration

E_e = electric field applied across detector element.

In terms of τ_{Ai} and R_r, Z_h becomes

$$Z_h = \frac{n_i^2}{bw}\left(\frac{\mu_e}{qtn_o^3}\right)^{1/2}\left(\frac{n_o}{2\tau_{Ai}} + R_r\right)^{-1}\left(\frac{P}{A}\right)^{1/2}$$

where n_i = intrinsic carrier concentration

P = electrical power dissipated in detector.

Background-limited performance can thus be achieved with materials and devices that satisfy this second inequality at temperatures consistent with satisfaction of the first inequality.

2. Extrinsic Photoconductive Detectors

In this case, the dopant ionization energy, E_d, determines the cutoff wavelength, λ_c

$$\lambda_c = \frac{hc}{E_d} \quad .$$

The first inequality becomes

$$B(N_d - N_a)t \frac{N_c}{g_c} \exp\left(-\frac{E_d}{kT}\right) << n\Phi_b,$$

where B = recombination coefficient

N_d = donor concentration

N_a = acceptor concentration

N_c = conduction-band density of states

g_c = generation rate of carriers in conduction band.

Since the left side of this inequality grows exponentially as the temperature increases, we can determine an upper bound for the operating temperature of the detector.

For an n-type extrinsic photoconductor, we assume that

$$\Delta n >> n_o \ ,$$

so that

$$AR = \frac{w^2}{qt\mu_e \Delta n}$$

and

$$\Delta n = \frac{\eta \Phi_b \tau_e}{t} \quad .$$

Then the second inequality becomes

$$G^2 AR >> \frac{kT}{q^2 \eta \Phi_b}$$

or

$$G^2 \frac{w^2}{\mu_e \tau_e} >> \frac{kT}{q} \quad ,$$

where $$\tau_e = [B(n_o + N_d)]^{-1} \quad .$$

If a device can be constructed such that G, w, N_e, and τ_e satisfy this inequality at a temperature less than or equal to the maximum temperature determined by the first inequality, then background-limited performance can be achieved.

3. Photovoltaic Detectors

For photovoltaic detectors, the dark current is expressed as

$$I_d = \frac{kT}{qR} \exp\left(\frac{qV}{\beta KT}\right)$$

where V is the applied voltage and β is a numerical factor which depends upon the nature of the material junction in the detector. For a Schottky barrier, $\beta = 1$; for a p-n junction, $1 \leq \beta < 2$. The photovoltaic gain is 1, and the first inequality becomes

$$\frac{kT}{q^2RA} \exp \frac{qV}{\beta kT} << n\Phi_b$$

or

$$nRA \exp \frac{-qV}{\beta kT} >> \frac{kT}{q^2\Phi_b} \quad .$$

The second inequality becomes

$$nRA << \frac{kT}{q^2\Phi_b} \quad .$$

We see that both inequalities require the maximization of RA. The work of Melngailis and Harman [Ref. 2] and Long [Ref. 1] has shown that the maximum value of RA for a p-n junction is obtained when a p^+-p, metal-semiconductor back contact is used. Then

$$\max\ (RA) = \frac{kTp_{po}\tau_e}{q^2Bn_i^2} \ ,$$

where P_{po} = equilibrium hole concentration in the p-type region

n_i = intrinsic carrier concentration

B = distance from p-n junction to the back contact.

This maximum value assumes that B is much smaller than the carrier diffusion length. The two inequalities thus become

$$\frac{np_{po}\tau_e}{Bn_i^2} \exp\left(-\frac{qV}{\beta kT}\right) >> \frac{1}{\Phi_b}$$

and

$$\frac{np_{po}\tau_e}{Bn_i^2} >> \frac{1}{\Phi_b} \quad .$$

Background-limited performance can be obta. ·d when material and device characteristics satisfy these inequalities.

G. DEPENDENCE OF BACKGROUND-LIMITED SPECTRAL DETECTIVITY

Since the detector material determines cut-off wavelength, λ_{co}, of the detector, the dependence of D^*_λ(BLIP) upon the cut-off wavelength is of interest. At first glance, since

$$D^*(\text{BLIP}) = \frac{\eta^{1/2}\lambda}{hc(u\Phi_b)^{1/2}}$$

it appears that D^*_λ(BLIP) varies linearly with wavelength. However, both η and Φ_b may be dependent upon the wavelength. We shall consider only the variation of Φ_b with λ_{co} here.

For a blackbody radiator at temperature T, the power radiated per unit surface area per unit wavelength (W cm^{-2} μm^{-1}) is

$$W_\lambda = \frac{2\pi hc^2}{\lambda^5}\left(e^{hc/\lambda kT}-1\right)^{-1} .$$

If N_λ is the photon emission rate per unit surface area per unit wavelength and E_λ is the energy of a photon of wavelength λ, then

$$\int_0^\infty W_\lambda d\lambda = \int_0^\infty N_\lambda E_\lambda d\lambda$$

and

$$N_\lambda = \frac{2\pi c}{\lambda^4}\left(e^{hc/\lambda kT}-1\right)^{-1} .$$

We define the background flux, $\Phi_b(\lambda_{co}, T)$, as the flux of photons of wavelength less than λ_{co} from a blackbody of temperature T. Hence

$$\Phi_b(\lambda_{co},T) = \int_o^{\lambda_{co}} N_\lambda(T)\, d\lambda$$

$$= \int_o^{\lambda_{co}} \frac{2\pi c}{\lambda^4} \left(e^{hc/\lambda kT}-1\right)^{-1} d\lambda \quad .$$

This integral can be cast in the form $\int \frac{x^2 dx}{e^{bx}-1}$; it can be evaluated using tabulated values of the Debye and Riemann zeta functions.

Using T = 300°K

N = 1

u = 4 (photoconductive case),

we find Φ_b and D^*_λ(BLIP) as functions of λ_{co}:

$\lambda_{co}(\mu m)$	$\Phi_b(cm^{-2}sec^{-1})$	D^*_λ (BLIP)$(cmHz^{1/2}W^{-1})$
5.0	$0.040X10^{15}$	$19.73X10^{10}$
6.0	0.391	7.586
8.0	1.981	4.494
10.0	4.672	3.658
12.4	8.531	3.356
15.0	12.745	3.322
20.0	19.522	3.579
30.0	27.871	4.492
∞	40.192	∞

The values for D^*_λ (BLIP) in both the photoconductive (PC) and photovoltaic (PV) mode are plotted in Figure III-6.

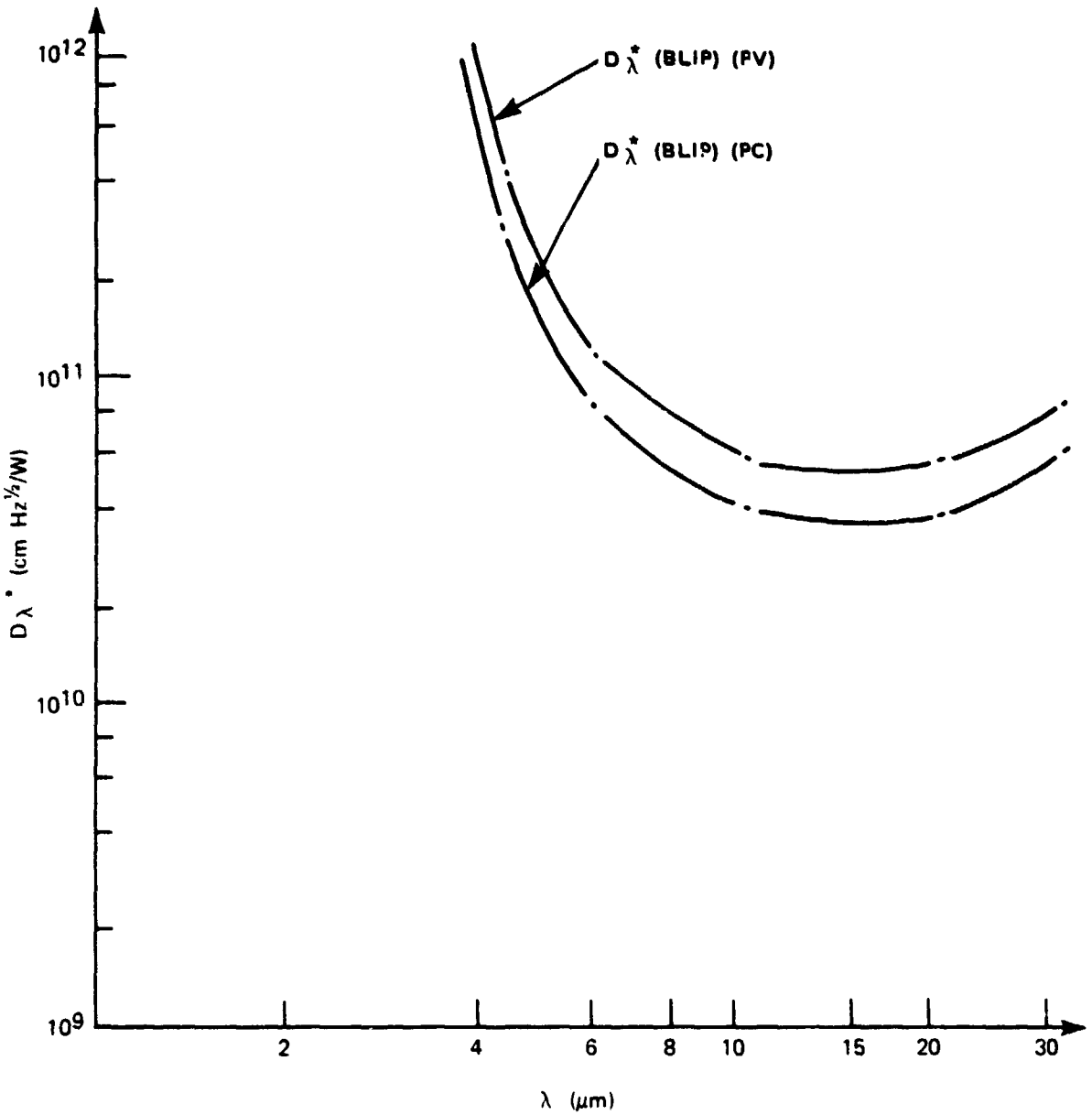

FIGURE III-6. SPECTRAL DETECTIVITY AS A FUNCTION OF WAVELENGTH FOR BACKGROUND-LIMITED DETECTORS

H. SIMPLE SENSITIVITY ANALYSIS OF SPECTRAL DETECTIVITY

In earlier discussion, we have expressed the spectral detectivities of photoconductive and photovoltaic devices as follows:

$$D^*_\lambda\ (PC) = \frac{\eta\lambda}{2hc}\left[\eta\Phi_b + \frac{P_o t}{\tau_h} + \frac{kTt\ (nb + p)\ \mu_h}{\left[(\mu_e + \mu_h)\ \tau_h E f(Z_h)\right]^2}\right]^{1/2}$$

$$D^*_\lambda\ (PV) = \frac{\eta\lambda}{\sqrt{2}\ hc}\left[\eta\Phi_b + \frac{bn_{po}}{\tau_e}\left(1 + \exp\frac{qV}{\beta kT}\right)\right]^{-1/2} .$$

Let us perform the following simplications:

- Ignore Johnson noise,
- Replace distance parameters b and t by w,
- Replace carrier concentrations by ρ,
- Replace lifetimes by τ, and
- Assume V is zero in the photovoltaic case.

We may then write the detectivities in a common, simple form:

$$D^*_\lambda = \frac{\eta\lambda}{hc\sqrt{u}}\left[\eta\Phi_b + \frac{w\rho}{\tau}\right]^{-1/2}$$

where u is 4 for the photoconductive case and 2 for the photovoltaic. Since the background-limited spectral detectivity is given by

$$D^*_\lambda\ (BLIP) = \frac{\eta\lambda_{co}}{hc\sqrt{un\Phi_b}} ,$$

we may write the ratio of the detectivities as

$$\frac{D^*_\lambda\ (BLIP)}{D^*_\lambda} = \frac{\lambda_{co}}{\lambda}\sqrt{1 + \frac{w\rho}{\eta\Phi_b\tau}} .$$

If we take D^*_λ to have its maximum value at the cut-off wavelength, then the minimum value of the detectivity ratio occurs at the point of closest approach of the detectivity curves and is given by

$$\min \left[\frac{D^*_\lambda \text{ (BLIP)}}{D^*_\lambda} \right] = \sqrt{1 + \frac{w\rho}{\eta \Phi_b \tau}} \quad .$$

We may easily tabulate the value of this ratio as a function of the value of $\left(\frac{\rho}{\tau}\right)$ in units of $\left(\frac{\eta \Phi_b}{w}\right)$:

$\frac{\rho}{\tau}$ $\left(\eta\Phi_{b/w} \text{ units}\right)$	$\min \left[\frac{D^*_\lambda \text{(BLIP)}}{D_\lambda} \right]$
0.0	1.0000
0.025	1.0124
0.25	1.1180
0.5	1.2247
1.0	1.4142
1.5	1.5811
2.0	1.7321
2.5	1.8708
5.0	2.4495
10.0	3.3166
15.0	4.0000
20.0	4.5826
25.0	5.0990
125.0	11.2250
250.0	15.8430
2.5×10^3	50.0100
2.5×10^4	158.1170
2.5×10^5	500.0010
2.5×10^6	1581.1391
2.5×10^7	5000.0001

We see that D^*_λ will be within 50 percent of D^*_λ (BLIP) if

$$\frac{\rho}{\tau} \leq 3 \frac{\eta \Phi_b}{W} \quad .$$

Some data for InSb indicate that this approach or a simple modification of it may be applied to evaluate existing materials. However, these data were drawn from several sources in the literature and must be evaluated for consistency. A systematic effort to gather consistent data on many materials is necessary.

I. DEVICE PERFORMANCE

Using the spectral detectivity as a measure of device performance, Figures III-7 through III-11 show the response of devices constructed from various materials. The following points should be noted:

- State-of-the-art processing provides isolated examples of high-performance materials.
- Cooling to liquid-nitrogen temperatures is required to obtain high detectivity.
- The data shown are for single detectors; the performance of detector arrays of uniform response is not discussed.
- Significant deviation from background-limited performance is seen at wavelengths below 3 μm.
- The fine structure of the HgCdTe curve for x = 0.18 is poorly understood.
- The long-wavelength tail of the Si:Mg curve is also not well understood; it may be related to the interaction of crystal defects and impurities.

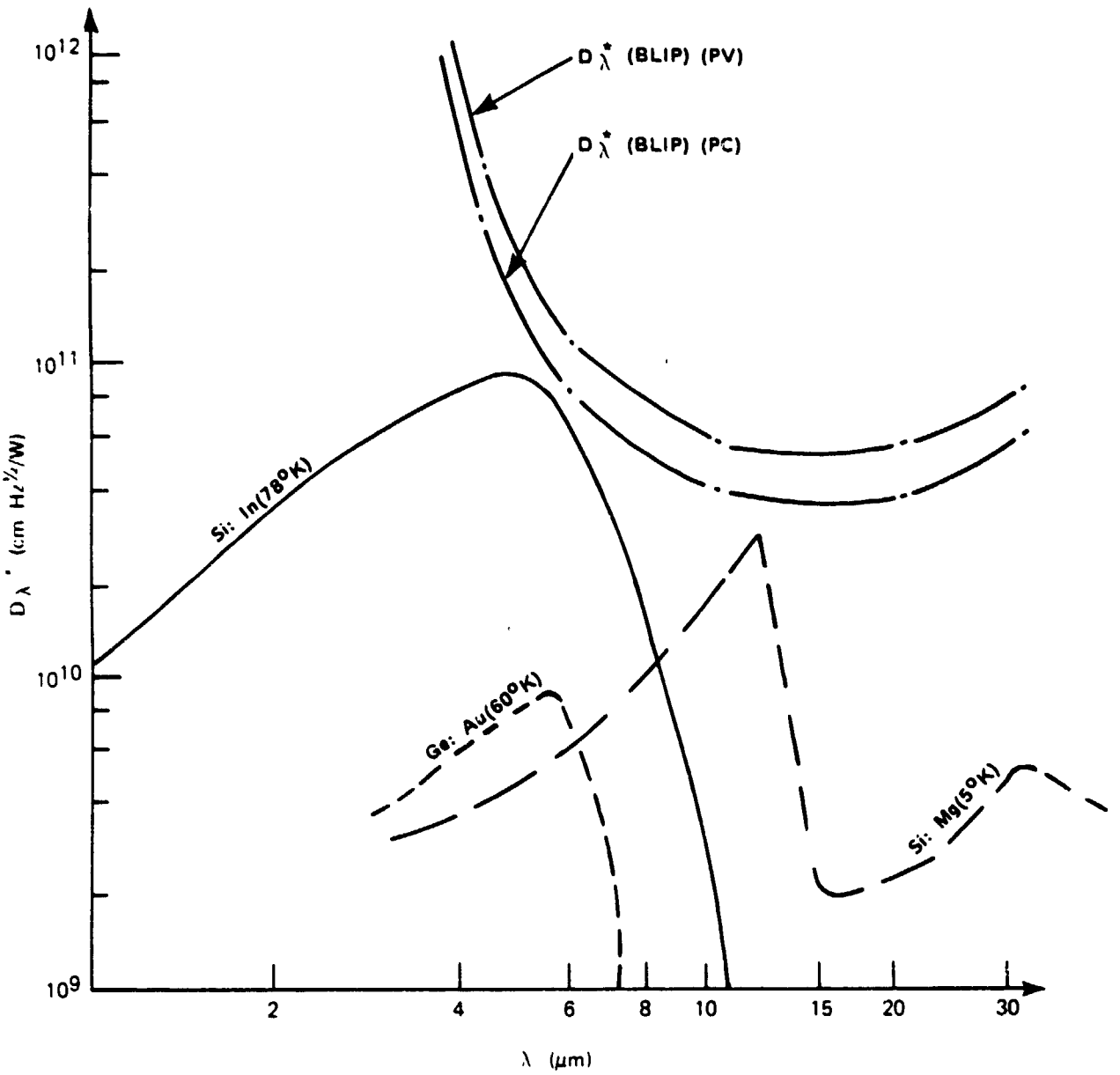

FIGURE III-7. SPECTRAL DETECTIVITY AS A FUNCTION OF WAVELENGTH FOR DOPED SILICON AND GERMANIUM

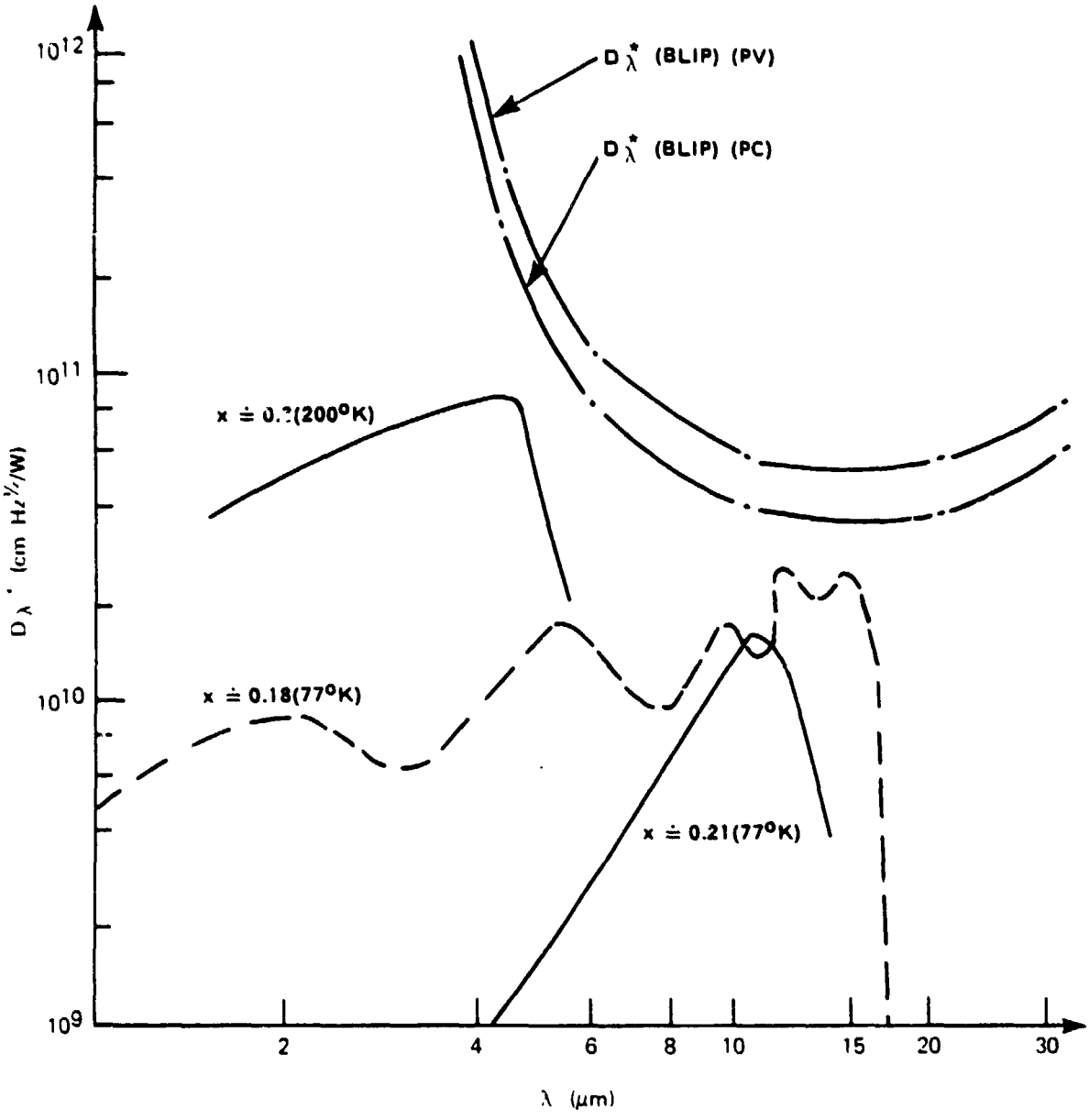

FIGURE III-8. SPECTRAL DETECTIVITY AS A FUNCTION OF WAVELENGTH FOR HgCdTe

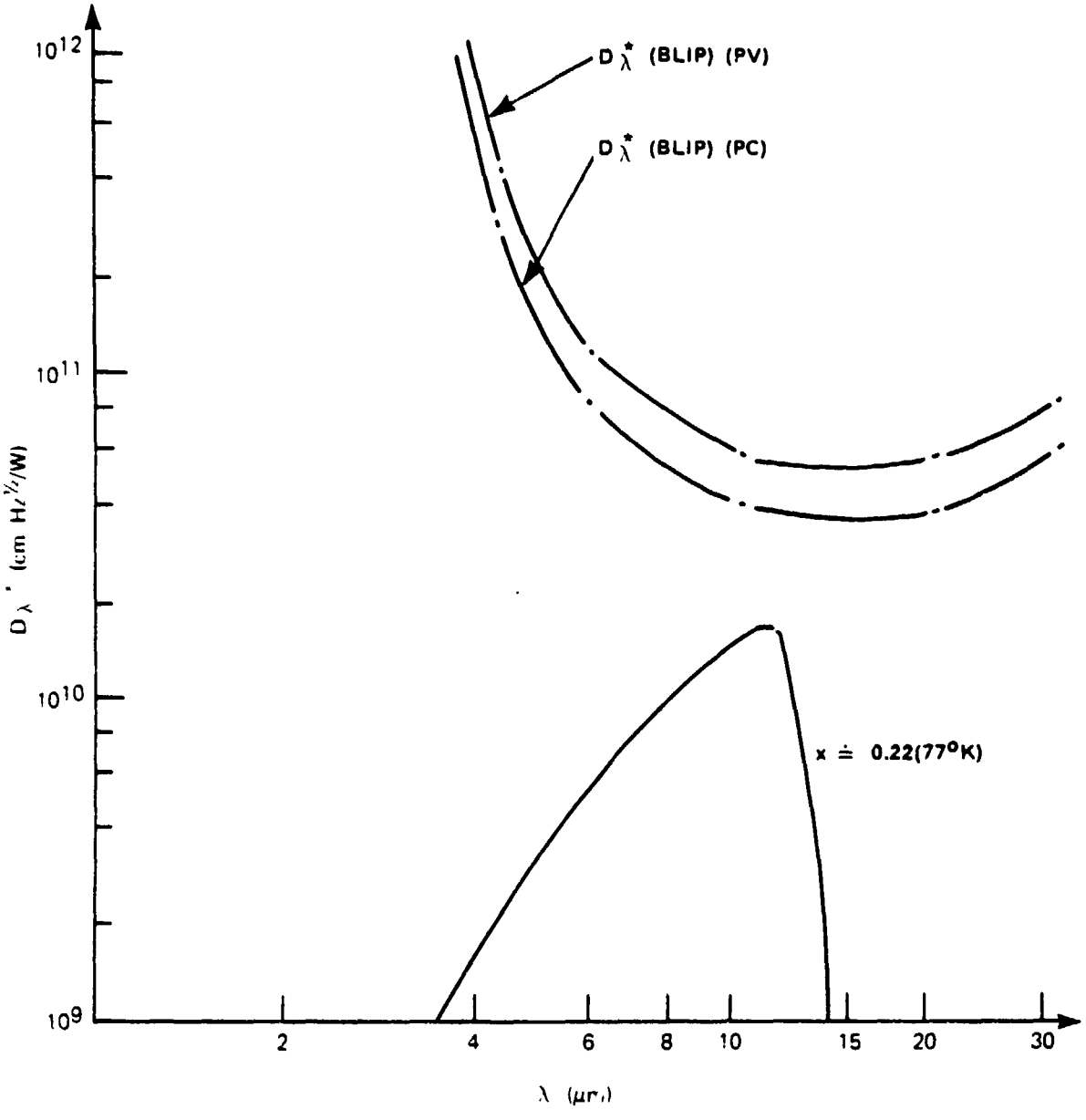

FIGURE III-9. SPECTRAL DETECTIVITY AS A FUNCTION OF WAVELENGTH FOR PbSnTe

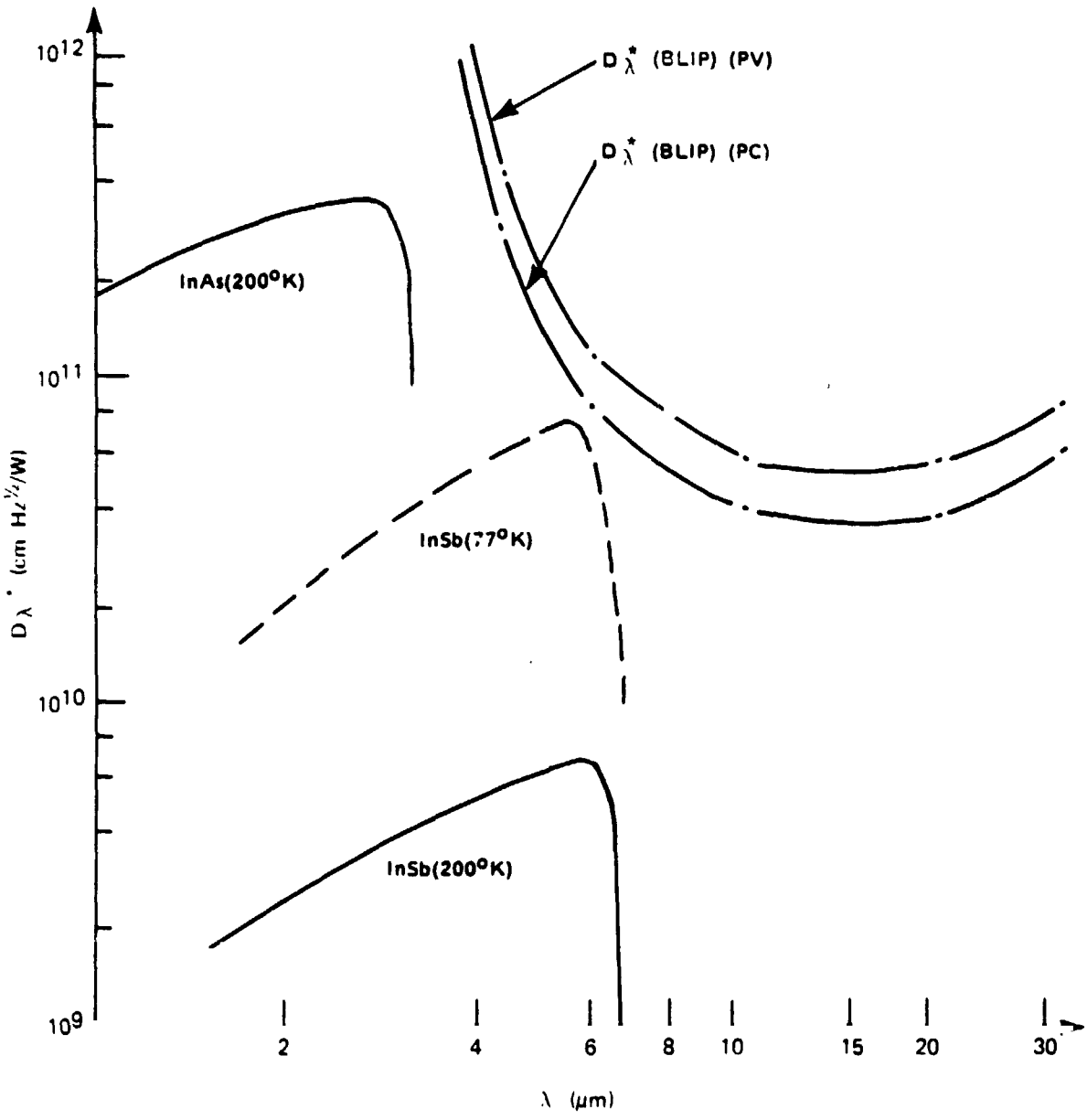

FIGURE III-10. SPECTRAL DETECTIVITY AS A FUNCTION OF WAVELENGTH FOR InSb AND InAs

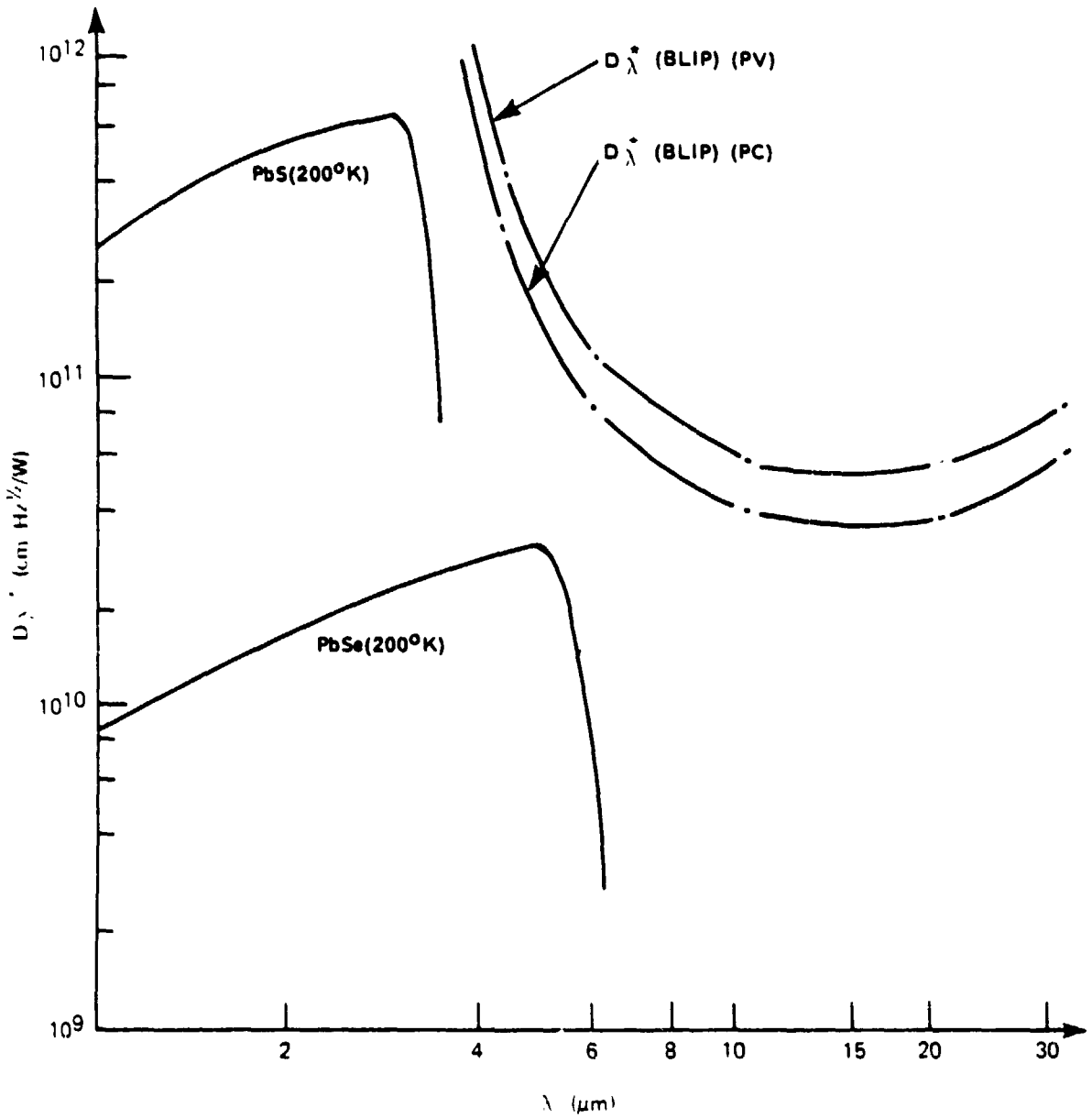

FIGURE III-11. SPECTRAL DETECTIVITY AS A FUNCTION OF WAVELENGTH FOR PbSe AND PbS

J. MATERIAL STRUCTURE AND DEVICE PERFORMANCE

Given the astounding improvement in the performance of solid-state devices over the past 30 years and the great proliferation of their applications, one might expect that the relation between material structure and device performance would rest upon a well-formed physical theory. This is, however, simply not the case today. An extensive body of knowledge does exist, but it is not systematic and it fails to touch upon many relevant questions.

It is very important to give some coherence to our current knowledge of the relation between structure and performance because further improvements in solid-state technology require much more precise control of material behavior than is now possible. High-speed, ultra-sensitive detectors require materials with impurity concentrations at least 100 times lower than those currently attainable. They also require great reduction in the concentration of crystal-structure defects.

In the absence of a comprehensive physical theory, the best alternative approach is to attempt a correlation of a semiconductor's electronic and structural characteristics. The important electronic parameters are properties of the population of charge carriers: concentration, mobility, and lifetime. The material parameters of interest are the crystal-defect density, the impurity and dopant concentrations, and the compositional homogeneity. Many sorts of crystal defects may be identified, and the principal types are discussed elsewhere in this report; their common trait is a disruption of the crystal's periodic internal geometry. Impurity and dopant concentrations simply refer to the number of extraneous atoms found per unit volume of the crystal. These extraneous atoms are generally termed impurities; if they are purposely injected into the structure, in order to provide a smaller energy gap for radiation absorption, they are called dopants. The final material parameter, compositional homogeneity, denotes the degree to which the atoms of a small part of a compound semiconductor conform to the definite stoichiometric proportions of the entire sample.

We next consider how each of the carrier properties is likely to be affected by each of the structural parameters. Carrier concentration should show spatial nonuniformity as one moves from regions of low crystal-defect density to regions of high crystal-defect density. Similar nonuniformity may be expected as a result of compositional inhomogenities. However, it is not yet possible to give a more precise description of the size of these effects, the spatial scale on which they occur, or their consequences for the photon detection process. The effects of impurity or dopant levels are better understood: if the impurity donates an electron at an energy level within the intrinsic bandgap, the thermal excitation of free electrons into the conduction band will be facilitated. If the impurity level can accept an electron, the thermal excitation of electrons from the valence band to the impurity level will be facilitated and more holes will be generated in the valence band.

Carrier mobility generally decreases with increasing concentration of defects or impurities. In effect, both of these departures from ideal crystal structure impede the movement of charge carriers by creating potential barriers which decrease the modes of free propagation available to the carriers. Compositional inhomogeneities create similar barriers, but little data on such effects are currently available.

Carrier lifetime shows a variable dependence upon crystal-defect concentration. In germanium, the lifetime decreases with increasing defect concentration at high levels of imperfection, but increases with increasing defect concentration at low levels of imperfection. This arises from an intimate relation between crystal defects and impurities; impurities appear to collect at crystal flaws under certain conditions, thus giving large portions of the bulk crystal a lower impurity concentration. This effect is poorly understood. If crystal-structure defects, compositional inhomogeneities and impurities prolong the carrier lifetime by isolating carriers from oppositely charged carriers, then these imperfections are known as "traps"; if they shorten the lifetime by facilitating the reunion of oppositely charged carriers, they are known as "recombination centers."

This discussion shows that we have some idea of the trends in the relation between material structure and electronic properties, but we are as yet in no position to determine electronic parameters by precise control of the complex structural chemistry of semiconductors.

K. CURRENT DRIVING FORCES IN DETECTOR DESIGN

Although many factors contribute to decisions regarding detector design, we may identify several dominant goals which will influence design during the 1980s:

- An increase in number of array elements
- A decrease in size of array elements
- Utilization of detector in staring, rather than scanning, mode
- Integration of detector array with charge-coupled devices (CCDs).

Increasing the number of detector elements allows detection of weaker signals, while decreasing element size improves the spatial resolution of the detector. Staring at a scene allows signal integration and thus raises the signal-to-noise ratio. Coupling the detector array to a CCD in the focal plane allows information in each array element to be read quickly and also makes possible fast and efficient image processing in the focal plane.

These design goals require an improved understanding of the physical properties of detector materials. Increasing the number of interconnected array elements will make uniformity of elements desirable. Casting ever smaller elements is likely to increase the importance of interfacial effects and demand precise control of material behavior. Furthermore, since the detector and signal-processing portions of an integrated array may often be made from different materials, the mechanical and electronic properties of these materials will be of great interest, particularly in the vicinity of a junction.

IV. METHODS AND PROBLEMS OF CRYSTAL GROWTH

Any IR detector is limited primarily by the care and control that was exercised in the growth of the basic material. Detector elements are so small that thermal and mass transport fluctuations at even a microscopic level can seriously degrade the device performance. This chapter offers a brief look at the processes involved in the common techniques of crystal growth.

A. CRYSTAL GROWTH

Crystal growth is one manifestation of the process of solidification. It represents a phase change on the part of a substance from a state of lower order to one of higher order. This process occurs as a result of temperature reduction (extraction of kinetic energy) and/or pressure increase. Either process allows the internal short range attractive forces between particles to become stronger relative to the kinetic barrier. The individual particles, which had relatively free movement in the gaseous state (confined only by the container) and liquid state (confined by the flexible boundaries of the liquid), are for the most part restricted to submicroscopic volumes in a solid. If the arrangement of the particles in the solid is random and isotropic, the solid is amorphous; if the arrangement has periodicity along well defined coordinate axes, the solid is crystalline. For a perfect crystal, the periodicity holds throughout the volume of the substance with no discontinuities. The total potential energy of such a structure is a minimum at a given temperature. However, this single crystal form is usually not found in very large structures. For substances that do have a crystalline phase, their composition is normally polycrystalline, made up of many small individual crystals oriented at

random. This is true because the final configuration is the result of a time evolutionary process conducted over a large spatial volume. At the instant of solidification, the local conditions vary considerably from point to point. This variation leads to a variety of crystal defects.

B. CRYSTAL DEFECTS

A full description of crystal structure and defects is far beyond the scope of this report. Instead, a few simplifications can provide a meaningful basis of understanding. Take, for example, a two-dimensional analog of crystal structure. In this model the crystal is viewed as an array of points representing atoms, each radiating four appendages. Each appendage of a point, when matched with an identical appendage from another point, forms a bond locking the two points together. A regular or symmetric structure is built up by joining many of these points together with four bonds for each point. Such a two-dimensional structure is pictured in Figure IV-1a. Inside a structure like this, an imaginary observer at any interior point would observe surroundings identical to those of an observer located at other points that are displaced from the first point by a distance equal to an integer multiplied by a constant. The value of this constant depends on the direction of displacement. It is this nonisotropic periodicity that defines a crystal and gives rise to its important properties.

A disruption of the periodicity will significantly alter the properties of the material. One such disruption is found at the boundaries of the crystal. As seen in Figure IV-1a, the boundary is characterized by dangling bonds. Since each bond represents an electromagnetic force, the electrical properties near the edge of each crystal are different from those in the interior. An additional disruption arises from the fact that the bonds are not rigid. There is a certain amount of elasticity, which permits vibrational movement of the atoms relative to one another without becoming completely dissociated. These vibrations arise from thermal, mechanical, or electromagnetic stimulation by outside forces.

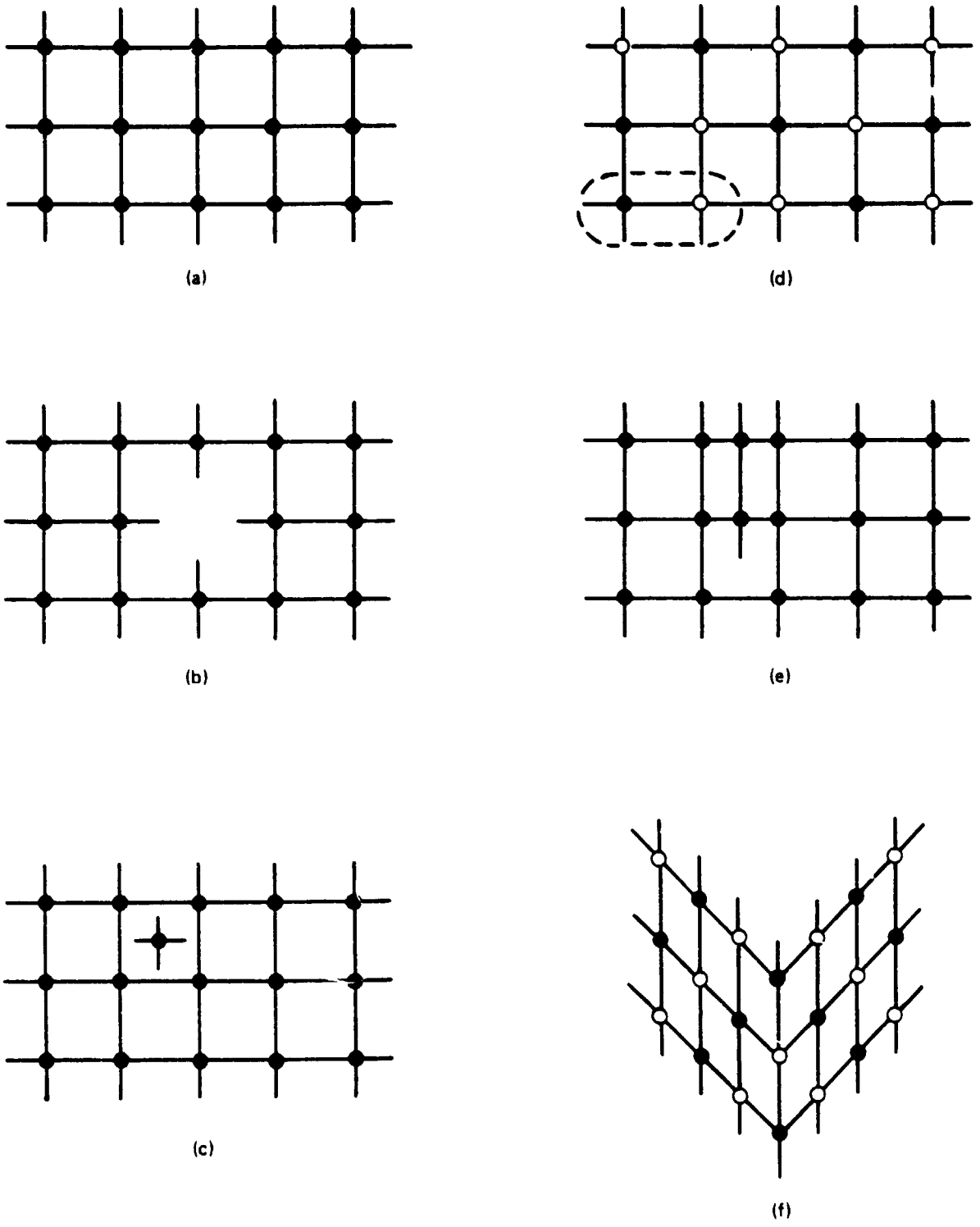

FIGURE IV-1. CRYSTAL LATTICE CONFIGURATIONS

The above describes fundamental limitations to the periodicity of any structure. Other disruptions are less fundamental and are known as defects. Defects can range from zero to three dimensions in character. The zero-dimensional point defects are of several types. If a lattice site is missing an atom, as shown in Figure IV-1b, it is known as a vacancy. If, instead, an atom is found in the spatial volume between lattice sites, as shown in Figure IV-1c, it forms an interstitial. These isolated point defects are characterized by a definite energy of formation. This energy arises from local thermal fluctuations at the time of crystallization with a probability of formation given by

$$\text{probability of formation} \propto \exp\left[-E_f/kT\right]$$

where E_f is the formation energy and depends on the type of defect. The probability of formation increases with the temperature at which solidification occurs. This indicates that crystallization processes that can be accomplished at lower temperatures are more desirable. In addition, once a point defect is formed it is relatively mobile, depending on the ambient temperature of the lattice. The probability of moving to a different site has the same dependence as the probability of formation with E_m, the energy of displacement, substituting for E_f. E_f is typically a few electron volts in magnitude while E_m may be only a few tenths. In this motion through the lattice, point defects may meet and collect or "condense" into clusters of many point defects, which can act as the source of different and more widespread defects.

In the previous discussion, the two-dimensional model consisted of only a crystal containing a single atomic species. The list of point defects for crystals formed from more than one atomic species is augmented by those defects formed when an unwanted impurity substitutes for a regular lattice or acts as an interstitial, or when the ordering of species is interchanged as shown in Figure IV-1d. The fact that point defects are so easily formed means that they can probably never be completely eliminated. Their presence must provide the fundamental limitations on the electronic behavior of crystals, such as charge carrier mobility and lifetime. Except

when present in large clusters such as silicon swirls, their presence is not readily available to direct methods of detection, making it difficult to make direct correlation between electronic behavior and point defect concentration.

The description of point defects was facilitated with the aid of a two-dimensional model. Higher dimensional defects require the extension of this model to three dimensions. It is necessary to imagine that the two-dimensional lattice is repeated indefinitely in the direction perpendicular to the paper. If a shear force is applied to a block of this material it may at some level exceed the elasticity available in the inter-atomic bonds. Slippage may occur along one plane of atoms, and a new equilibrium position may be achieved in which a half plane of atoms, terminated with dangling bonds at the slippage plane, is found squeezed between two other planes. These adjacent planes have all their bonds paired but are under some tension. An end view of this configuration, known as an edge dislocation, is represented by Figure IV-1e. The shear forces that produce these edge dislocations can arise from stresses produced by high thermal gradients in a cooling solid, by unmatched thermal expansion coefficients of the solid and any container, or by unmatched lattice parameters of an epitaxially grown layer and the substrate. The chain of dangling bonds forming the boundary of an edge dislocation represents an electronic anomaly in the lattice. This can act as a trap for charge carriers or it can pin impurity atoms, producing various undesirable consequences for carrier lifetime and mobility. Even in the best of crystals the density of edge dislocations or similar defects is typically 10^3 cm^{-2}.

Two types of defects that do not necessarily result in dangling bonds are the screw dislocation and the lattice twin. Screw dislocations are characterized by a spiral ramp type of transition from one crystal plane to the next rather than by one layer placed upon the other. The origin of these dislocations is not clearly understood, although some mechanisms have been suggested arising from an array of edge dislocations or point defects. Twin boundaries arise from slight lattice displacements due to stress. The lattice structure on one side of the twin plane is the mirror image

of the other. An example is shown in Figure IV-1b. Twinning is more likely to occur at low temperatures than slips producing edge dislocations. The major effects of screw dislocations and twins are altered directional properties and strain energies.

The next levels of defects, consisting of grain boundaries (a surface of dislocations forming the boundary between crystals of different orientation) and occlusions of impurities, are disastrous for any detector material. These result from complete lack of control over the crystal growth interface. Various other types of defects can be identified and labeled, but they differ from those already mentioned in shape rather than substance. They are generated from the same general conditions as the others.

C. THE CRYSTAL GROWTH INTERFACE

The interface is the instantaneous boundary between the advancing solid and the substance that provides the raw material to fuel the crystal's growth. This substance may be a gas, a liquid, or even another solid. If the nutrient or noncrystalline phase is a liquid or gas, its particles are relatively free to move about. That is, their kinetic energy exceeds the attractive potential energy existing at the crystal boundary. If some mechanism exists to reduce a particle's energy, it may become trapped in the potential well of the lattice and thus become a part of it. Conservation of energy requires that the kinetic energy lost by the newly bound particle appear elsewhere. If the energy is lost due to an inelastic collision with the lattice, it appears as a phonon (lattice vibration) and contributes to heating the lattice. If the energy is lost from an inelastic collision with another particle in the noncrystalline phase, it contributes to an increase in temperature of that material. A reverse process can also occur. If an energetic particle in the nutrient material strikes the lattice with sufficient force, it may break the bonds of a lattice atom and thus increase the amount of the noncrystalline phase. In truth, both processes occur simultaneously. If the former process is more frequent, we have net crystal growth; if the latter predominates, we have a net crystal shrinkage due to melting, vaporization, or dissolution.

The growth process requires that thermal energy be transferred out of the system. In controlled growth processes the heat is transferred out of the cooled solid phase. The overall growth rate of the crystalline phase depends on its heat transport properties (governed by thermal conductivity and the temperature gradient present) and on the mass and thermal transport properties of the noncrystalline phase.

The above discussion described the solidification process simply but adequately. However, it does not introduce any mechanism that controls crystal perfection. This can best be described by looking at an equilibrium situation consisting of a perfect crystal in contact with a liquid (or gas) of the same composition held at the melting (or sublimination) temperature of the material. At equilibrium there will be no net gain or loss of material by the solid phase. On a local microscopic level, however, there will be a continuous process in which particles become attached to and released from the interface. These two processes balance each other. The particles of the noncrystal phase may attach themselves to the solid interface in various configurations, some of which do not preserve the perfect crystal structure. However, since the perfect crystal represents an energy minimum, the attractive bonds are strongest in that configuration. Therefore in the equilibrium state, with its continual process of attachment and detachment driven by the statistical variation of kinetic energy, the bonds most readily broken are those that could preserve defects. Even so, at any given time there are likely to be a number of point defects. It is however, the process of reversibility in the equilibrium situation that keeps these defects to a minimum.

As the process is moved away from equilibrium by extracting heat from the system, both processes still occur. However, the attachment process happens at a greater rate so that the solid solidification front advances and freezes in any defects. Although the bonds corresponding to a perfect crystal may be strongest, they may not be the ones most likely to be formed at a given instant. It is only in the equilibrium reversible process that they are overwhelmingly dominant. In a dynamic growth situation, the percentage of defects is therefore more likely to increase as the growth rate increases. Another factor that leads to more defects is higher temperature.

The higher temperature means that there is a greater fraction of particles with energy sufficient to break the stronger bonds of the newly created atoms forming the perfect structure.

The above situation is comparatively simple in that it deals only with a pure substance. It does indicate that more defects are likely to occur at higher temperatures and higher growth rates. For realistic systems having several components and with less control over temperature and composition, the environment at the interface is much more complex. For the pure substance, the perfect crystal represented a minimum energy state. As such, there was a definite overall tendency to produce such a state. In the case of mixed substances, the desired composition is likely to represent only a local energy minimum, which can be achieved within a very narrow range of control variables such as temperature, pressure, and composition. Even if these variables are well controlled on a macroscopic level, normal statistical fluctuations will set limitations on the level of microhomogeneity that can be achieved.

Although there are numerous problems peculiar to each individual system, an examination of a few example cases can illustrate major common difficulties.

Case 1: Growth of a Pure Single Element Crystal

In this hypothetical pure substance we need not worry about segregation of components. The only imperfections that can arise are structural defects. The most simple defects are point defects and may be of two types: vacancies or interstitials. They are illustrated in Figures IV-1b and IV-1c. Each of these defects is characterized by an energy of formation E_f and an energy of mobility E_m. As discussed previously, the probability of formation and mobility are related to the temperature by

$$P_f \alpha \exp [-E_f/kT]$$

$$P_m \alpha \exp [-E_m/kT] .$$

The mobility of the point defects can lead to several consequences. If both vacancies and interstitials are present in the lattice, the random meeting

of two opposites will annihilate each other. If two vacancies or two interstitials join, the defect energy will be reduced since there will be fewer unpaired bonds. Thus, there is a tendency to form large defect structures from coalescing or condensed point defects. Depending on the density of such defects and on the nature of the device, the condensation may or may not be desirable. The mobility of the defects is enhanced by annealing the crystal at some elevated temperature. This process can result in defect annihilation, condensation, or it can cause defects to move to the surface and disappear. If the condensation is not desirable, the crystal can be rapidly cooled, thus freezing the individual point defects in place.

Case 2: Growth of a Single Element Crystal With Impurity

The impurity may be intentional or unintentional. Unintentional additives arise due to limitations of the purification process, or they enter later as contaminants diffusing out of a container in high temperature crystallization steps. Intentional additives are dopants, which must be incorporated uniformly in bulk crystal growth or perhaps gradiently in epitaxial growths. In either case, the dopant atoms may substitute for the predominant specie in the host lattice or enter into interstitial locations. The crystal grower now has the dual goal of achieving structural perfection along with compositional uniformity.

For dopants there is frequently a limitation to the maximum amount of solute material which can be incorporated into the host crystal. The solubility of the dopant is usually greater in the liquid mixture than in the solid. At some concentration the interaction forces between the dopant atoms pass a threshold of nucleation at which point they form precipitated aggregates rather than remain as isolated individuals. These large aggregates can apply significant stress to the cooled lattice, introducing various structural defects.

Even at concentrations below the solubility limit, the equilibrium concentration of solute differs between the crystal and noncrystal phase. For example, at equilibrium the solid and liquid concentrations of the solute at the interface are related by $k_o = C_S/C_I$. For $k_o < 1$, some of the solute is continually rejected from being incorporated in the solid phase. This, left

alone, produces a concentration gradient on the liquid side of the solid-liquid interface. At this point one of two distinct processes can occur. If a mechanism exists that can mix the liquid "infinitely" fast, the rejected solute can be dispersed uniformly throughout the remainder of the liquid. Under this mechanism the concentration of the solute in the remaining liquid increased steadily. This increase is reflected by a parallel increase, but still at a lower level, in the concentration in the solid. In the total absence of any such fast mixing mechanism the concentration of the solute in the interface boundary will increase until it reaches a point at which the diffusive loss of solute into the bulk liquid is equally balanced by the gain as it is rejected from the solid. At this stage the concentration of the solute in the solid will maintain a steady value until nearly all the liquid has solidified, at which point there will be a sharp increase. Curves representing the two processes are shown in Figure IV-2. Since it is the equilibrium (or segregation) coefficient K_0 and the concentration in the liquid phase that determine the concentration in the solid, any variations of solute concentration along the liquid side of the interface caused by currents of any kind will be reproduced to some scale in the solid.

The above discussion was concerned with the intentional incorporation of dopant. The other side of the coin deals with undesirable contaminants. For any growth processes in which hot material (especially molten) is in contact with a container, there is always, to some extent, diffusion of undesirable species from the container to the growing crystal. These contaminants typically will be distributed nonuniformly. For applications in which impurity concentrations of the order of parts per billion or less are required, the contributions of the unwanted contaminants can be serious.

Case 3: Growth of Multicomponent Alloys and Compounds

Heavily doped materials would also have problems similar to those of this case, while this case would include all the problems of the other two cases.

The complexity involved in describing the processes leading to crystallization of multicomponent materials arises from the multitude of interatomic forces that are present. These forces are of different strengths

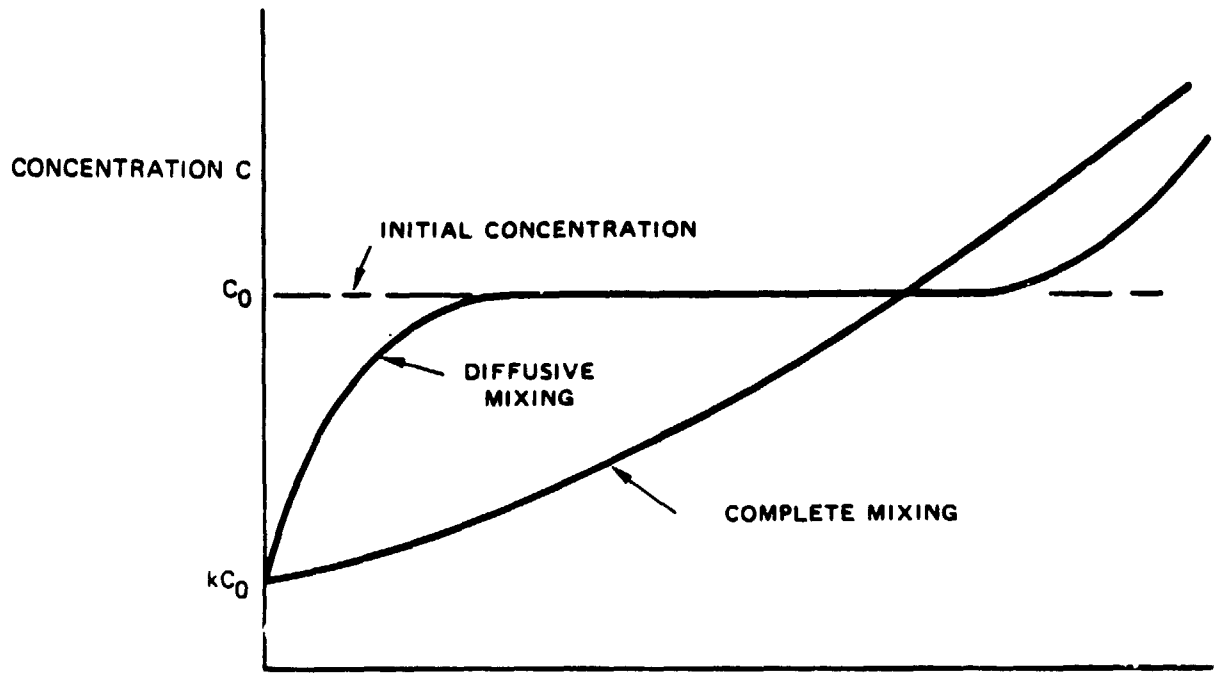

FIGURE IV-2. MECHANISMS OF MIXING

and different ranges. Whereas single element materials normally provide only three distinct phases with sharp thermodynamic boundaries (as represented on temperature-pressure curves), multicomponent materials can provide a wide variety of phases depending on composition. The thermodynamic boundaries of these phases include wide transition ranges.

If it is desired to form a crystal having a specific chemical composition, one might hope to achieve this by starting with, for example, a melt of the same composition. In doing so it would be necessary in the course of the solidification to deal with any or all of the following phenomena.

1. Component Volatility

At the elevated temperatures required in preparing the melt, one or more of the constituents might possess a high vapor pressure in equilibrium with the melt. If the ambient atmosphere does not balance this pressure, material will be transported from the melt and thus alter its composition.

2. Component Segregation

For a given material composition there is frequently a wide temperature gap between the point at which solidification begins and where it ends. These points are the liquidus and solidus points respectively. For two completely miscible components A and B, these points will vary with composition as shown in Figure IV-3. Suppose we have a melt of composition A_oB_o and want to form a crystalline solid of the same composition. Referring to the phase diagram, we note the following problem. At equilibrium the composition of the liquid and solid phases are different at the interface. To achieve the desired solid composition in a quasi-equilibrium fashion, one can lower the temperature at the interface slowly through T_o until the desired compositional melting point T_s is achieved. In the course of this process, a solid having a higher melting temperature is formed whose composition is richer in component B. Thus component A is rejected into the melt, producing a liquid boundary layer with a higher concentration of A. As the temperature lowers further, the concentration of A in the solid increases but is still below that of the bulk of the melt. Meanwhile, the concentration of A in the liquid boundary layer increases. Having reached the desired temperature T_s, the composition of the solid is A_oB_o as wished and that of the liquid boundary layer is A_1B_1. A density gradient near the interface might be represented by the concentration of A as shown in Figure IV-4a.

In the absence of any mixing forces other than diffusion, the growth front can be propagated through the liquid. This assumes that the rate of diffusion of A in the melt is matched by the rate of rejection at the moving interface. Several processes may act to destroy this equilibrium. The liquidus temperature corresponding to the varying composition of the melt near the interface may be represented by the curve of Figure IV-4b. If the temperature gradient into the melt, as shown by G_1, produces a temperature at any point exceeding the liquidus except at the controlled interface, growth will proceed producing the desired composition. However, if the gradient is less, as shown by G_2, the material near the interface is undercooled (constitutional super-cooling). This provides an unstable situation in which the planar interface can break down into rapidly advancing solid

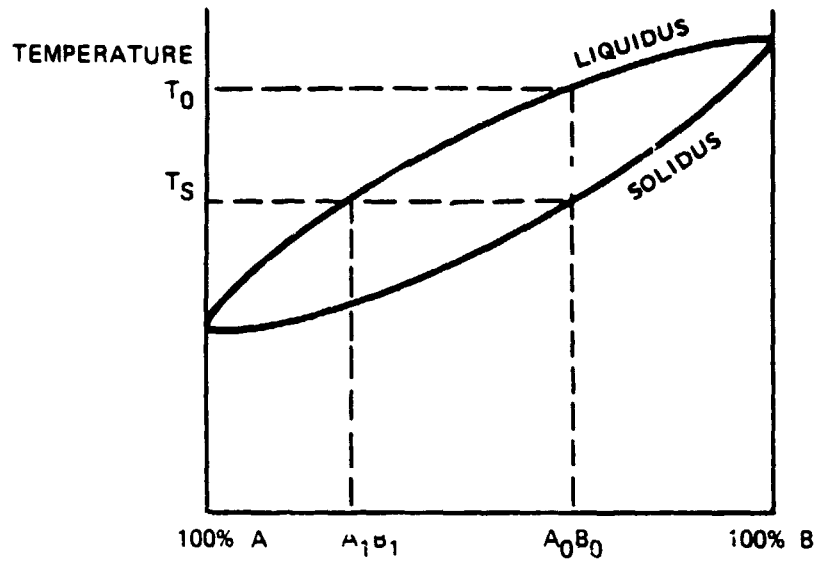

FIGURE IV-3. BINARY PHASE DIAGRAM

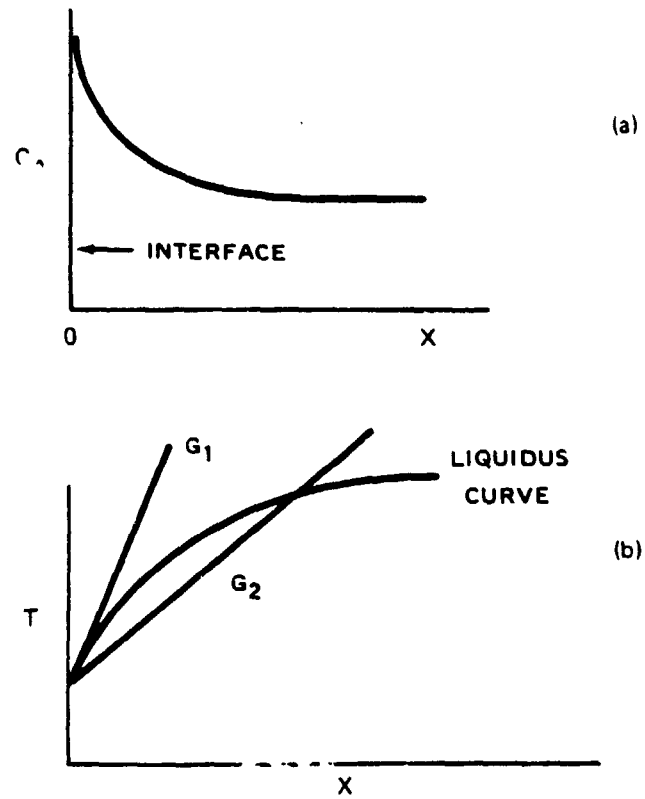

FIGURE IV-4. GROWTH INTERFACE

projections having one composition that surround liquid channels having a different composition. The resulting crystal is inhomogeneous.

Another growth phenomenon of concern is the problem of faceting. In most processes involving controlled growth a seed crystal is used to initiate growth along a specific axis. If an isothermal plane can be maintained perpendicular to this axis, growth will usually be achieved in this plane. However, most isothermals have some curvature, bringing them parallel to other crystallographic planes. These other planes may have slightly different growth properties, such as different solidification temperature and different segregation coefficients for impurities and solutes. If growth progresses along these other axes, compositional inhomogeneity will result.

D. INSTABILITY MECHANISMS

The environment in which crystal growth takes place is rarely quiescent. Not only is it necessary to first establish the proper conditions to produce a suitable crystal, but it is also essential to design a system that does not become imbalanced by the random perturbations that are bound to occur. These random perturbations (which at the very least can arise from statistical fluctuations) in themselves are the source of many microinhomogeneities. More important, however, is their effect on the system as a whole. If the system reacts in a manner that tends to restore the initial unperturbed state, the system is stable On the other hand, if the system reacts in such a way as to reinforce the perturbation, the system is unstable. If the conditions that gave rise to the stability are maintained, a flow pattern will develop. Some sources of instability that may be present in crystal growing operations are examined.

1. Gravity Driven Convection

The gravitational force on any volume of fluid is proportional to the amount of mass in that volume, i.e., the mass density. Most fluids expand when heated, thus decreasing their density. Therefore, for a pure substance the gravitational force is greater in the cooler portion of the fluid. Figures IV-5a through 5c show three types of heating configurations. The arrows

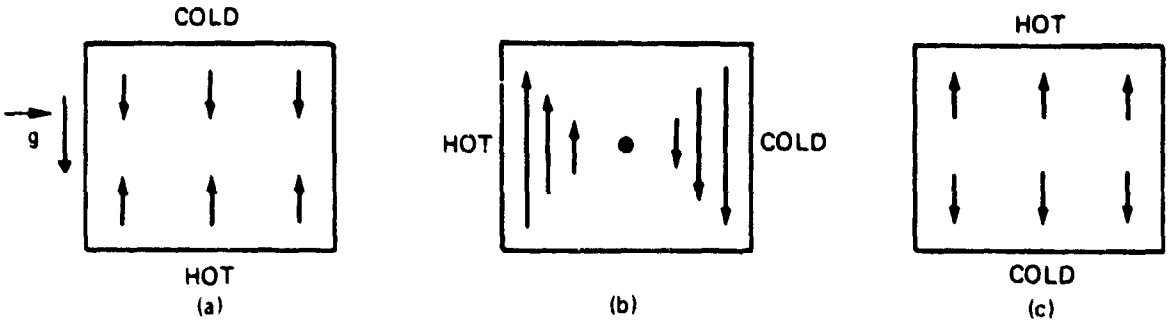

FIGURE IV-5. BUOYANCY-DRIVEN CONVECTION

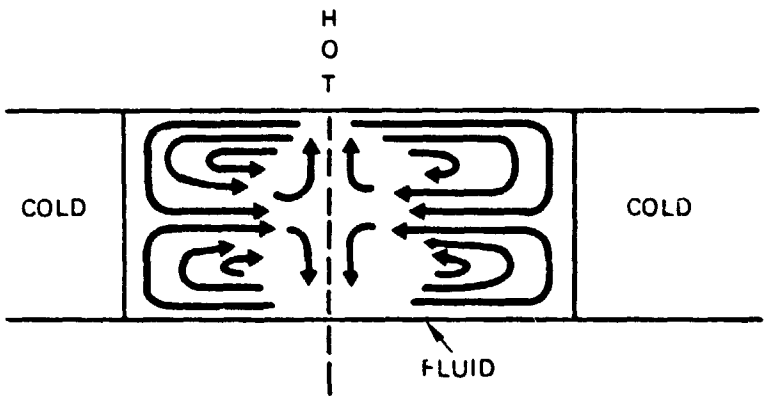

FIGURE IV-6. MARANGONI-DRIVEN CONVECTION

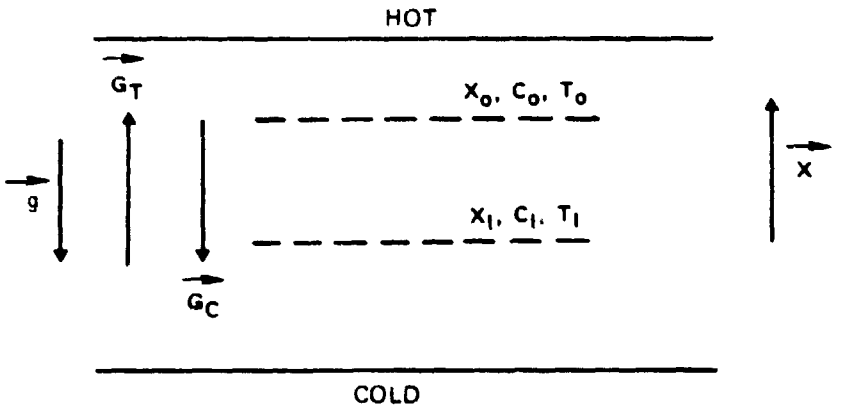

FIGURE IV-7. DOUBLE-DIFFUSIVE CONVECTION

represent the gravitational force on a volume of fluid "normalized" to the value at a point midway between the hot and cold plates. Figure IV-5a pictures a potentially unstable situation. Any perturbation will set in motion a flow pattern that causes the colder layers to sink to the bottom. The thermal gradient required to initiate flow depends on properties of the material, such as viscosity, thermal expansion coefficient, thermal diffusivity, and some dimensional parameter. Figure IV-5b represents a case in which flow always occurs. In both cases a and b two types of flow are possible: steady state flow or time varying flow. Figure IV-5c represents a configuration in which any perturbed fluid element will return to its initial position after some damped oscillatory behavior.

2. Marangoni Convection

This type of convective flow is present in liquids having a free surface (the interface between a liquid and gas or between two liquids). The driving force for this type of convective flow is the surface tension. For systems where surface tension gradients are present (due to thermal gradients or concentration gradients) there is a tendency for the system to maximize surface tension (minimize surface area). This is accomplished by mass flow in the surface layers from a region of low surface tension to one of high surface tension. If the conditions that produced the gradient are maintained, a continuous flow pattern is produced. The surface flows are transmitted some distance into the bulk of the fluid by viscous shear forces. An example of Marangoni flow is illustrated in Figure IV-6. Surface tension a substantial driving force, and for some configurations, Marangoni convection is dominant over gravity-driven convection.

3. Double Diffusive Convection

This convective mechanism arises from the presence of two diffusive species, e.g., thermal and mass. In all circumstances the thermal diffusion speed is much greater than mass diffusion. Figure IV-7 illustrates a configuration similar to some in crystal growth. A fluid has a linear concentration gradient G_c pointing down and a linear thermal gradient G_T pointing up. The gravitational vector $\vec{g}$ points down. The concentration gradient G_c

is that of the less dense constituent. Assume a mass density at any point x relative to that at point x_o is given by

$$\rho(x) = \rho_o \left[1 - \beta_T G_T (x-x_o) - \beta_c G_c (x-x_o)\right]$$

$$= \rho_o \left[1 - (\beta_T G_T + \beta_c G_c) (x-x_o)\right] ,$$

where β_T and β_c are positive constants relating density to temperature and concentration differences. At first glance we might think that the configuration is stable if $\beta_T G_T + \beta_c G_c > 0$. This would ensure that the less dense mass is at the top, with no possibility of gravity driven (buoyancy) convection. This, however, does not take into account the dynamics involved in a perturbed situation. Assume a small volume of the fluid is displaced from position x_o to position x_1. In the course of the displacement, over a finite time interval, diffusive forces will try to equilibrate the displaced volume with its surroundings. The thermal diffusivity being so much faster, it can be assumed that upon reaching x_1 the temperature of the displaced fluid has reached T_1 while its concentration is still C_o. Thus its density at x_1 is now

$$\rho_D = \rho_o \left[1 - \beta_T G_T (x_1-x_o)\right]$$

while that of the surroundings is

$$\rho_s = \rho_o \left[1 - (\beta_T G_T + \beta_c G_c) (x_1-x_o)\right] .$$

The difference is

$$\Delta\rho = \rho_D - \rho_s = \rho_o \left[\beta_c G_c (x_1-x_o)\right]$$

$$> 0 \text{ since } x_1 < x_o \text{ and } G_c < 0.$$

Therefore the displaced fluid is denser than its surroundings and it will continue to fall. A similar analysis for a fluid element displaced upwards

would show that it would continue to rise. Both conditions represent instability. Although the linear gradients postulated in the example are not necessarily realistic, the example shows that the potential exists for this type of convective flow. Analysis for more complex gradients provides the criteria necessary for the instability to exist.

4. Additional Flow Instabilities

Other flow instabilities can be introduced by additional driving mechanisms. If rotation is used in pulling a crystal from a melt, convectional flow driven by centrifugal force is introduced. If RF heating is used on a metallic melt, there are magnetic body forces exerted on the induced currents.

E. GROWTH TECHNIQUES

Crystals are routinely prepared from a variety of starting materials in any of several phases. The method used for any specific composition is determined first by what is chemically and thermodynamically possible, then by quality and quantity of the product. The source material may be a liquid or vapor phase. Several growth mechanisms are described in general terms.

1. Czochralski Growth

This method involves "pulling" a solidified crystal slowly from a melt (Figure IV-8). A seed crystal of proper orientation is initially dipped into the molten batch and withdrawn slowly. Cooling through the seed and crystal holder permits a continuous process of solidification. The diameter of the crystal can be controlled by the pull rate. Since the growing crystal is not confined, structural defects caused by different expansion coefficients for crystal and container are eliminated. The crystal is rotated to enhance thermal uniformity across the growth interface and to aid in mixing any dopants added to the melt. This method of growth is fine for crystals which do not have volatile components. However, for materials having constituents with high vapor pressures, it is extremely difficult and prohibitively expensive to fabricate a sealed Czochralski

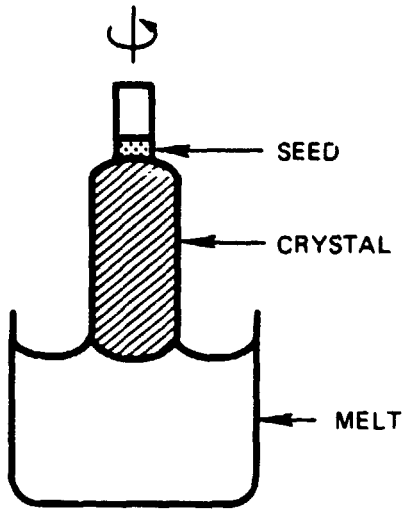

FIGURE IV-8. CZOCHRALSKI GROWTH

system to prevent loss of the volatile component. For materials with moderate vapor pressures a "liquid encapsulation" technique may be used which coats the surface of the melt and newly grown crystal with a low solubility substance to prevent loss of vapor. Limitations of this technique arise from the finite solubility of the encapsulation substance and from the loss of a free surface, a fact which can produce additional defects. Contamination of the melt by impurities in the crucible is a problem. High purity crucibles which minimize contamination are expensive and in some cases can only be used once.

2. Boat or Capsule Growth

Growth by this method involves confinement of the grown crystal in an open top vessel (boat) or in a sealed capsule. Two types of crystal growth are possible, normal freezing and zone melting. Normal freezing involves initially melting all of the starting material (with the possible exception of a seed crystal used to provide lattice orientation) and passing

the growth interface from one end of the material to the other by means of suitable cooling techniques. The process can be accomplished in either a horizontal or vertical configuration (Figure IV-9). For any multicomponent material, components may segregate at the interface. The presence of convective currents will distribute the rejected component to the bulk of the melt producing a longitudinal compositional variation. Convective currents are always present in the horizontal configuration. The gravitation driven convection may be suppressed by using a vertical configuration with the temperature gradient advancing upwards, which places the less dense fluid on top.

Rather than initially melting the complete sample, it is possible to melt only a narrow segment (Figure IV-10a) of the starting solid and pass this molten zone from one end to the other. Since the molten volume remains fixed throughout most of the process, there is less compositional variation due to segregation and convection transport. For some substances, zone melting is possible in a vertical configuration (Figure IV-10b) where it is known as a floating zone. This zone can be held, without benefit of confinement, suspended between two solid sections by virtue of surface tension.

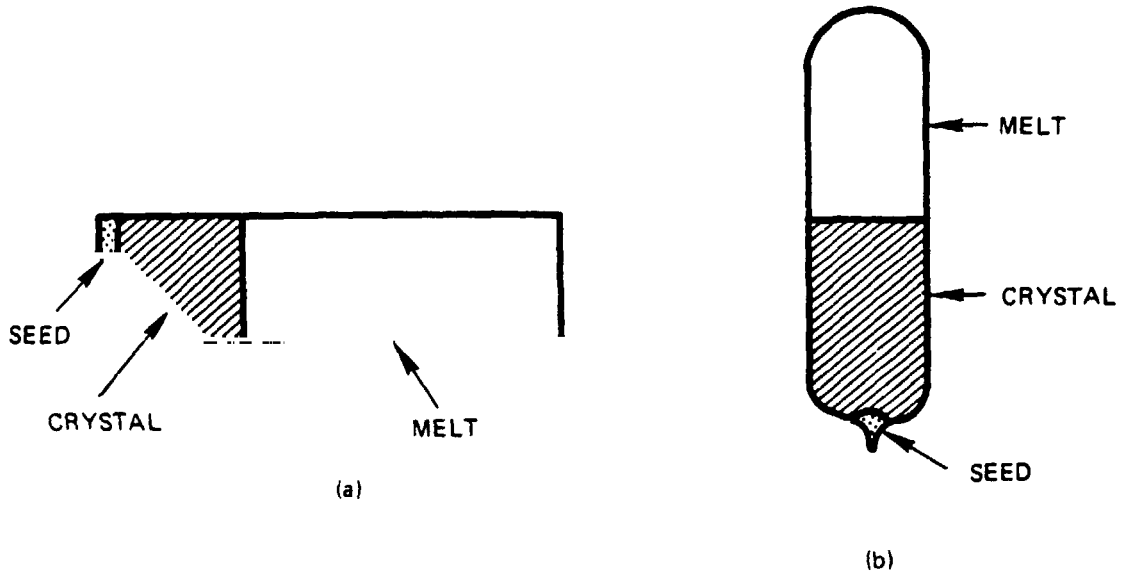

FIGURE IV-9. NORMAL FREEZING

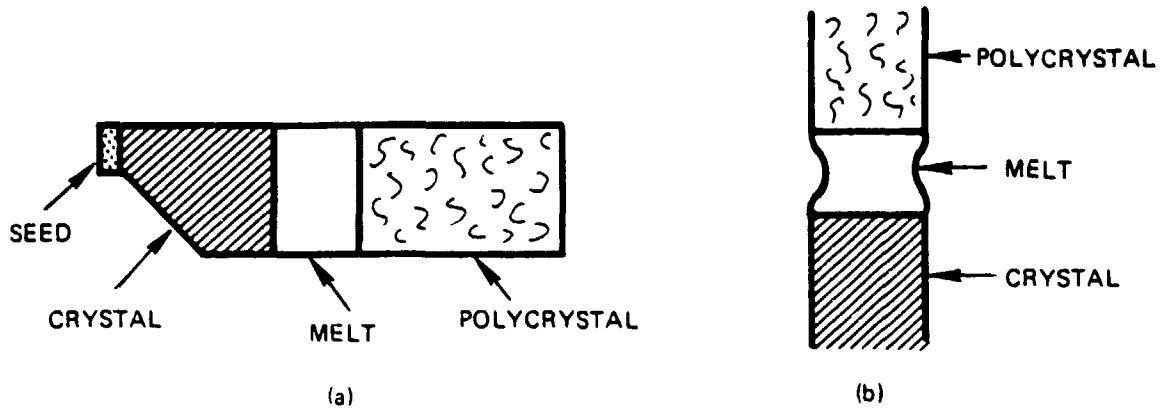

FIGURE IV-10. ZONE MELTING

This method, unlike the horizontal normal freezing and zone melting and the vertical normal freezing, keeps the hot reactive material away from container walls, which might otherwise lead to contamination and/or structural imperfections.

3. Growth From Solution

Growth of some crystals in bulk or as epitaxial layers (liquid phase epitaxy) may be achieved at temperatures lower than the melting point by dissolving them in a suitable solvent and then making the solution supersaturated by lowering the temperature or evaporating the solvent. Crystallization at lower temperatures produces fewer defects. In addition, for those materials whose melting point is too high to be practically achieved or for which the compound dissociates upon melting, solution growth may be the only viable method. Several limitations are involved in solution growth. The solvent may contaminate the crystal to an undesirable amount. Growth rates are typically very low, due to low solubilities of solute and/or low

transport rates of solute to the growth interface. For alloy materials the solvent may be an increased proportion of a low melting point component. Growth of the desired composition requires rigid temperature control to prevent solidification of an unwanted composition. In addition, the growth kinetics change as the solute is used up. Growth and compositional uniformity may be enhanced in many materials by passing a current through the substrate-liquid interface (electroepitaxy). This is an isothermal process in which the composition and growth rate are determined by the substrate composition, temperature, and applied current density.

4. Growth From a Vapor

Vapor phase methods are slow but may produce crystals of high purity and perfection. These crystals may be produced on a specific substrate or allowed to nucleate on the container walls. Some methods involve chemical vapor transport in which some of the crystal components are contained in a gaseous chemical compound and are released at the growth interface by a chemical reaction. Temperature and compositional control are most easily achieved via vapor methods.

V. POTENTIAL PROGRAM DIRECTIONS AND THRUSTS

The past several chapters have indicated a considerable uncertainty in the production of solid state crystals for infrared detectors. Although some success has been had with the growth of doped silicon crystals with a variety of cutoff wavelengths (see Fig. III-1), the selectivity, especially in the important atmospheric window between 8 and 14 microns, is not good. Binary detectors have also shown similar important limits. The ternary compounds, on the other hand, have shown theoretical promise over the full range of conditions. Their drawback has been in the inability to be produced in appropriate quality, quantity, and size to make complex detector arrays sensibly economic.

This effort at SPC was originally initiated to develop a case for the utility of a low gravity environment in alleviating or eliminating this problem of producing large, homogeneous, defect-free solid state detector crystals in a wide range of compositions and shapes. Instead we have confirmed, in a somewhat more quantitative fashion, one of the conclusions of the STAMP Committee,[1] that there is insufficient knowledge about the ground-based crystal growth of solid state detector materials to allow unique quantification of the contribution of reduced gravity-induced segregation and convection on crystal perfection. Questions as to why some of the crystals presently grown on earth have exemplary characteristics and how composition, temperature, geometry, and other factors combine to provide these "good" samples from amongst the bulk of poor material are not well understood, least of all in those ternary materials of particular interest.

---

[1] Materials Processing in Space, Report of the Committee on Scientific and Technological Aspects of Materials Processing in Space, Space Applications Board, Assembly of Engineering, National Research Council, NAS: Washington, D.C., 1978.

For this reason we have reviewed References 3, 4, 5, and 6 as reasonable representations of the state of activity in NASA and the military in the economic production of solid state detectors for infrared sensors. Although the four reference works do not cover all the activities in these types of materials, nor for that matter all the activities within NASA and the military, it is felt that they provide a sufficiently comprehensive base to allow a reasonably detailed investigative program to be laid out. This program would investigate all of the identified problems and make a first-level effort at identifying where, if anywhere, work is being carried out that addresses each of the problem areas. A more detailed assessment of how far along the state-of-the-art is in each problem area would have to take place in a workshop attended by representatives of each of the major solid state infrared detector crystal growing activities in the country. This effort is meant as an initial outline to guide their deliberations and to aid in further fleshing out of specific areas for priority investment.

To aid in this assessment, we have organized our discussions into the six areas shown in Figure V-1. The material combination discussion is essentially compositional. It looks at elemental, binary, ternary, and quarternary intrinsic combination and the unintentional and intentional impurities, contaminants, compensators, and dopants that alter their electrical performance. In the trends in fundamental properties, the basic thermal properties important to the growth mechanization and the more atomic properties important to electric performance are assessed. Thermal properties include phase diagrams, partial pressure, mass diffusivities, thermal conductivity, surface tension, etc., while atomic properties emphasize molecular weights, lattice constants, Fermi energies, and bandgap energies. Growth mechanizations deal with normal and zone melting, float zone melting, pulling from a crucible, liquid and vapor phase epitaxy, molecular beam epitaxy, and other of the newer mechanisms for controlling the growth process. Emphasis is placed on the controllability of axial and radial temperature gradients with size and shape, external pressure control, concentration gradient, and gravity effects inherent in the mechanization and the potentials in annealing cycles.

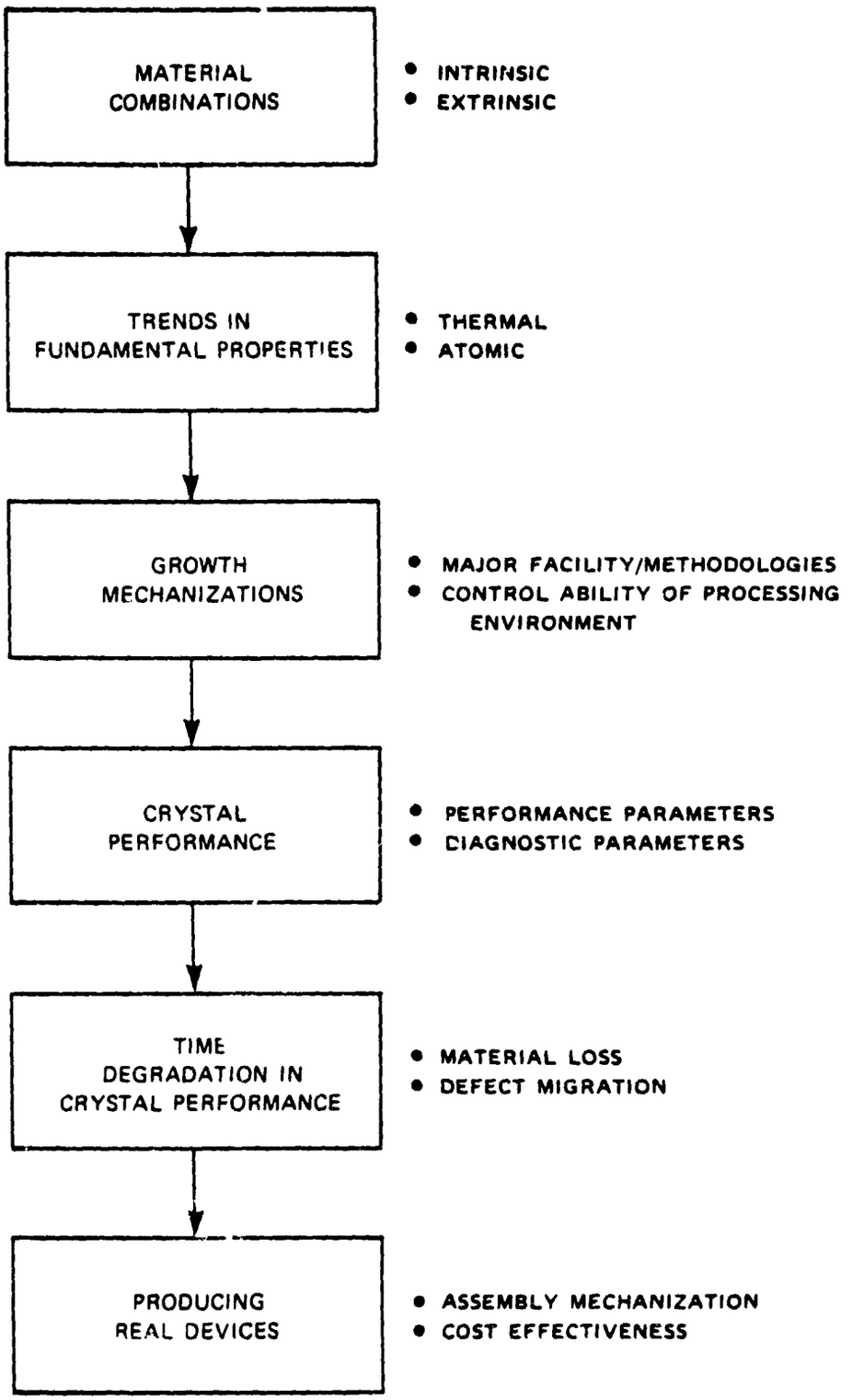

FIGURE V-1. FUNCTIONAL ORGANIZATION OF DISCUSSION

TABLE V-1. SELECTING MATERIAL COMBINATIONS

Intrinsic Combinations	Extrinsic Modifications
Elemental (Primarily IVs)	Irremovable Impurities
Binary (III-V, II-VI, IV-VI)	Containment Contaminants
Ternary	Compensators
Quaternary	Dopants

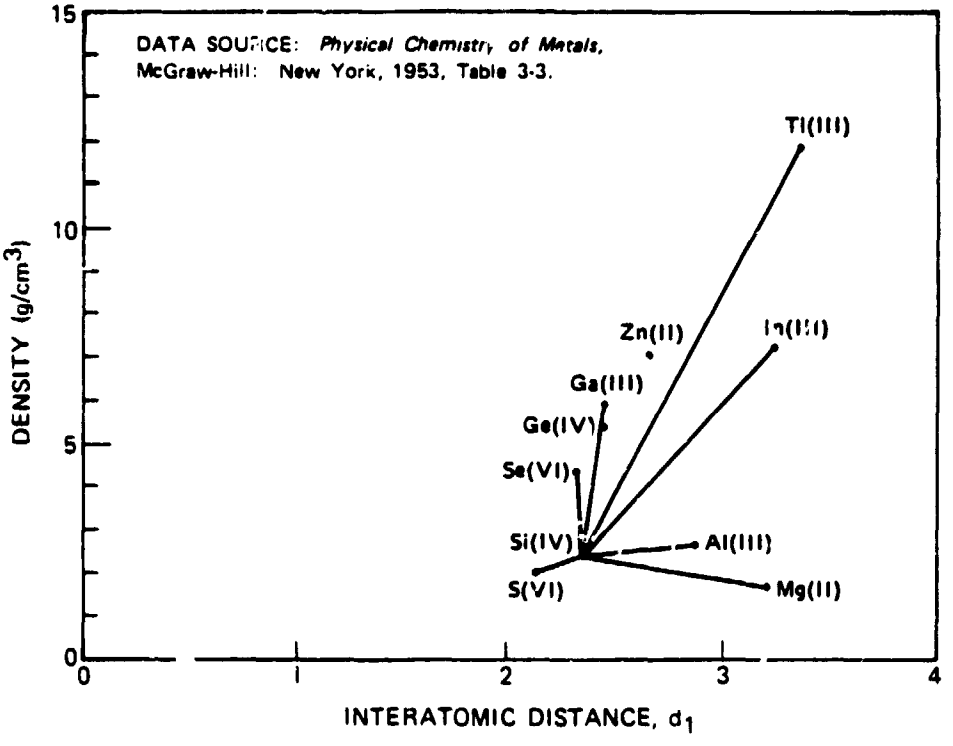

FIGURE V-2. DOPED ELEMENTAL OPTIONS

Crystal performance addresses the electrical properties important to understanding the device potentials and the diagnostic measurements necessary to assess material homogeneity and potentials for time delay in performance. Lifetime is given special emphasis, both due to compositional losses from component volatility or from chemical leaching by adjacent materials and due to defect migrations from edge effects or from adjacent materials and joints. The real problem, though, is in the total device preparation process. Mechanical sizing actions induce defects, and layering or junctioning activities can induce a variety of defects. The detection layer is then only a piece of the total system performance. Out of all of this, some attention must be given to cost effectiveness in terms of quantity production, simplicity, standardization, and automated validation.

A. SELECTING MATERIAL COMBINATIONS

In evaluating material combinations for IR detectors, it is convenient to separate intrinsic and extrinsic considerations, as shown in Table V-1. The number of elemental, binary, ternary, and quaternary combinations that make sense to try are rather finite. Many of these were displaye earlier in Figure III-1. In addition, the effects of impurities and additives also have to be considered.

1. Elemental, Binary, and Ternary Compounds

Figures V-2, V-3, and V-4 summarize the major possibilities. Silicon and germanium detectors have been extensively studied, with and without an array of dopants. As shown in Figure V-2, silicon has been doped with all of the appropriate III elements and several II and VI elements. Germanium has similarly been studied, but it provides even less span in cutoff wavelength number. Although there is much work that could be done (e.g., Ref. 3) to improve elemental detectors in terms of (1) larger sizes, (2) less contaminants in the initial load and from the growth processes containment, (3) less crystal defects, and (4) more homogeneous distributions of dopants and compensators, it is our feeling that it is more

important to look forward to the more flexible ternary compounds. Doped silicon and germanium have rigid limits in the cutoff wavelengths obtainable so that there is inherently less adaptability in terms of controlling the cutoff wavelengths within the narrow graded bands needed for the array detectors desired by NASA and the military.

The major options for binary and ternary detectors from III-V combinations is shown in Figure V-3. We have plotted density against interatomic distance as somewhat simplistic substitutes for the more complex effects of gravity-driven segregation and interelement diffusion or convection coefficients. GaAs and InSb, the two most popular of the III-V binaries in this context, are seen to be made from pairs of the most similar atoms. This means that they have less gravity-driven segregation and diffusion effects and tend to diffuse and convect relative to each other from thermal effects in comparable manners. Thus, these combinations should be the easiest to grow and should be the most free from defects and inhomogeneities due to non-controllable gravity and thermal effects. Comparing this with Figure III-1 shows that the cutoff wave length generally rises with a rise in the binary density. This implies that it should be important to investigate combinations with bismuth and/or thallium (Tl) to see if the cutoff wavelength is increased into the 8-14 micron atmospheric window. Once these additional binary compounds are investigated, then the InAsSb ternary could be used to finely divide up the 3-5 micron window and some ternary combination of InTlBi, InSbBi, TlSbBi, or InTlSb might be appropriate for finely breaking up the 8-14 micron window, without the high sensitivities shown at one end in the III-VI and IV-VI ternary compounds. Rockwell is already looking into the InAsSb ternary under an Air Force Contract and NASA had a Skylab experiment utilizing this material. The InGaSb compound also appears interesting. The InSbBi should be similarly producible if InBi produces higher cutoff wavelengths, but there may be some problems due to the lack of complete intersolubility between the two binaries. Ternary combinations using P, Al, or Tl may also have some problems in crystal growth stability. If they show desirable properties for particular uses, it might be necessary to go to low gravity processing for these materials to maximize the potential for crystal homogeneity.

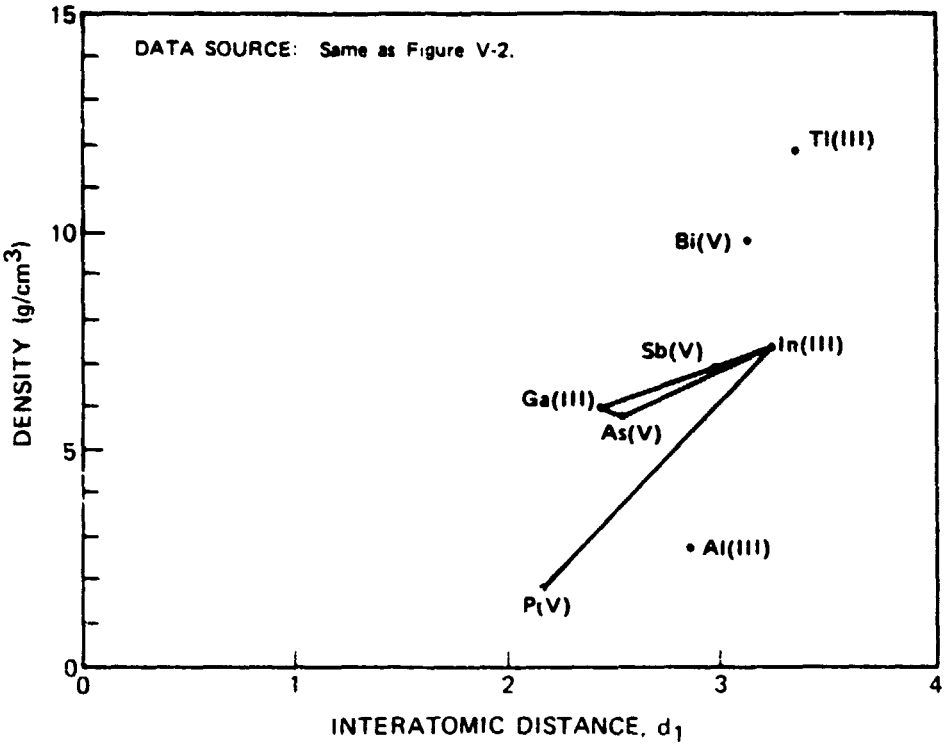

FIGURE V-3. III-V BINARY AND TERNARY COMPOUNDS OPTIONS

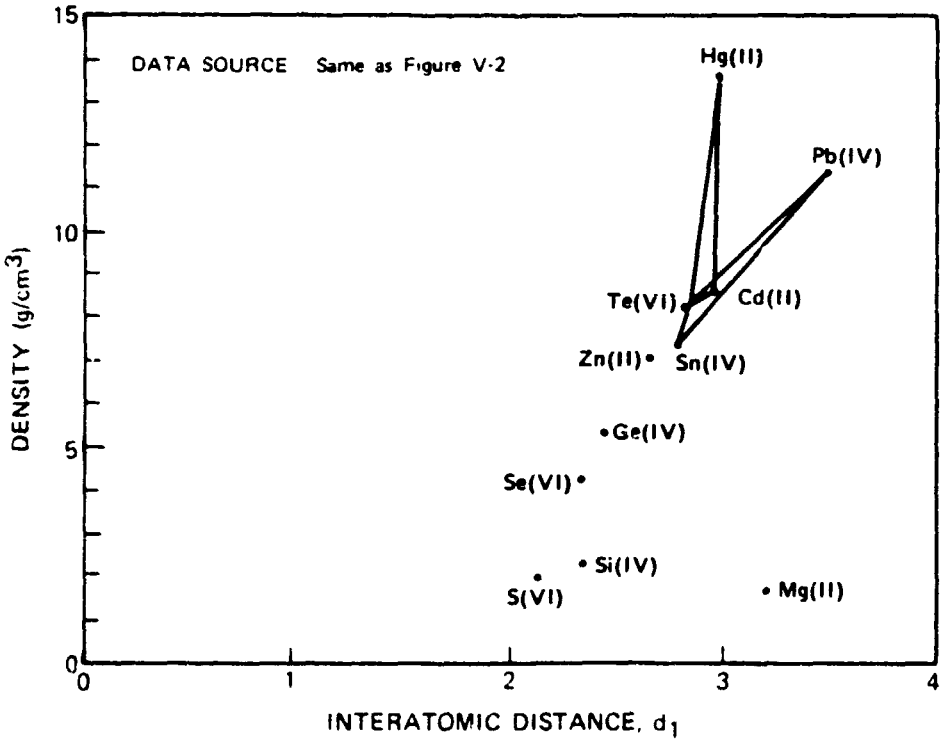

FIGURE V-4. II-VI AND IV-VI BINARY AND TERNARY COMPOUND OPTIONS

The II-VI and IV-VI compounds are shown in a similar simplistic manner in Figure V-4. The semi-metal characteristic of HgTe provides one driver for high cutoff wavelength (see Fig. III-2). The $Pb_{0.6}Sn_{0.4}Te$ combination provides another driver for high cutoff wavelength (Fig. III-3). Other combinations which might produce high cutoff wavelengths were not identified in this literature review, but may exist. The key is that the elements in the HgCdTe compound all have similar lattice parameters and similar diffusion processes in the melt stage. This gives it the greatest potential for earth-based crystal growth among these options. The PbTe and SnTe binaries also have similar lattice parameters, although it does not appear that way from the element data in Figure V-4. Both of these ternary materials (shown connected in Fig. V-4) appear to have potential, eventually, for low gravity processing due to the high density of the Hg and Pb components.

Carrying the assessments of Figure V-3 and V-4 further, it does not immediately appear that quaternary combinations have anything additional to offer. There are a lot of loose ends that need to be tied up before this could be made a conclusion.

In summary, then, the following recommendations can be made in terms of selecting major compounds for IR detector systems without considering nonremovable contaminants and the various compensators.

- Emphasis should be on ternary compound systems. Doped silicon or germanium and binary compounds may have particular application in specific wavelength regimes, but if the ternary production problems can be solved, then ternary compounds can cover these regimes plus many others not directly feasible from the doped elemental or binary systems. Quaternary systems, also, do not now show any particular advantage over ternary systems unless they can be shown to eliminate some processing time in ternary systems which has not to our knowledge been identified.
- In the far infrared from 3 to 50 μm, emphasis should be on $Hg_{1-x}Cd_xTe$ $InAs_{1-x}Sb_x$, $In_{1-x}Ga_xSb$, $Pb_{1-x}Sn_xTe$. HgCdTe can cover the full range but the volatility of Hg makes processing difficult and requires encapsulation to prevent Hg leaching and subsequent detector degradation. The same range can apparently be covered by utilizing the InAsSb or InGaSb combinations in the 3 to 5 μm regime and PbSnTe in the 5 to 50 μm regime.

The combination of these several ternary combinations eliminates some of the volatility problem, but perhaps trades it for other problems.

- In the visible and color infrared regime (0.4-3 μm), there is much spectral absorption detail for earth resources applications on renewable and nonrenewable resources, on water and oil pollution, and on atmospheric sounding. It would be appropriate to investigate ternary combinations in this regime also to replace doped silicon, and several binary compounds which generally have to be used with complex (and lossy) filtering or beam splitting arrangements in order to get fine spectral detail. Ternary combinations like $GaN_{1-x}As_x$ appear to cover the visible regime (0.4-0.7 μm). $Al_{1-x}In_xAs$ and $Hg_{1-x}Cd_xTe$ appear to cover the near infrared or color infrared regime (0.7-3 μm). This area appears to be particularly important to future NASA programs. All three materials have density variations which may necessitate low gravity processing. GaN has been difficult to process on earth.

It should be noted that a substantial majority of the NASA and military work is on HgCdTe combinations. There has been some free literature effort on PbSnTe combinations, and Rockwell is investigating InAsSb combinations for the Air Force (see Ref. 5). More specific assessments of particular combinations are the subject of the remainder of this report. We have not identified any significant activity on the use of ternary combinations in the visible and near-infrared regimes out to 3 μm. This should be an important area for NASA, but perhaps less important for the military. Need for this lower frequency regime is one of the major divergences between civilian and military requirements and could substantially impact the future Landsat missions for NOAA.

2. Impurities, Contaminants, Compensators, and Dopants

In keeping with our recommendation to stick with ternary combinations, we will restrict our discussion here to that area. All the base materials used for the ternary combinations suggested for study have some level of relatively irremovable impurities left over after the purification process is complete. These somewhat inherent impurities need to be understood, in particular relative to their contribution to the donor/acceptor situation in the ternary compound. Different impurities are present in each

of the three base materials, and the contributions of these impurities to performance uncertainties needs to be understood. Honeywell (see Ref. 6) is studying for NASA the effects of specific dopants on $Hg_{1-x}Cd_xTe$ combinations, where the dopants are used as compensators. How much of this compensation is needed to allow for defects due to natural impurities and how much is due to structural and stoichiometric defects due to the growth process is unknown. Hopefully it is small, as normally assumed. In addition, most of the growth processes provide opportunity for additional contamination due to the container, the pressurized atmosphere, or the carrier fluid. These impurities also need assessment through controlled experiments, with known, purposely added variations in all the impurities and contaminants identified with a particular material source and crystal growing technique. The Honeywell effort for NASA has been looking at copper, indium, phosphorus, iodine, and gold primarily as compensators.

In this area we recommend:

- A systematic study of the quantity of impurities and contaminants typical in each of the ternary combinations of interest. Crystals should then be grown which vary the quantity of each of the individual contaminants systematically in order to compare their relative contributions to overall detector performance.
- The Honeywell type of study on defect chemistry needs to be expanded to additional dopants and compensators and to additional ternary combinations.

B. MEASURING FUNDAMENTAL MATERIAL PROPERTIES

In order to understand the potential problems inherent in any crystal growth process, it is important to understand the fundamental thermal and atomic properties of the candidate materials (e.g., Table V-2). These thermal and atomic properties strongly influence the growth interface dynamics and the potential for defect or dislocation generation during this growth process.

The only systematic efforts presently funded in solid state detectors are the two efforts at McDonnell Douglas and Marquette University listed in Table V-3. Both efforts have tended to stress stoichiometric compositions,

whereas much of the present bulk and liquid phase epitaxial work is with the nonstoichiometric initial loads needed to allow for geometric restrictions on growth and for real melt dynamics. Other thermal properties are generally taken from an incomplete literature, aided by theoretical calculations. Similarly, the atomic properties of interest are not all available from experiments, and theoretical values are therefore relied upon.

TABLE V-2. ASSESSING TRENDS IN FUNDAMENTAL PROPERTIES

Thermal	Atomic
Phase Diagrams	Molecular Weight
Component Partial Pressures	Lattice Constants
Mass Diffusivities	Fermi Energies
Thermal Conductivity	Band Gaps
Surface Tension	
Viscosity	

TABLE V-3. PARTIAL SUMMARY OF ONGOING EFFORTS IN MEASURING FUNDAMENTAL PROPERTIES

Properties Measured	Sponsor	Company	Material	Additives	~FY80 $K
Phase diagrams, partial pressures	NASA/ MSFC	McDonnell Douglas	$Hg_{1-x}Cd_xTe$	Not Specific	
Phase diagrams, partial pressures	AF/OSR	Marquette	$Hg_{1-x}Cd_xTe$		40

From this we recommend that:

- Phase diagram and partial pressure measurements be expanded to include other ternary compounds and both stoichiometric and nonstoichiometric combinations. Since NASA is generally more space and earth resources oriented, NASA might usefully emphasize materials for the 0.4 to 3 μm regimes where the military is less interested and in compounds without the mercury, which tends to be lost under space pressures. This degrades performance, either from the material loss or from the contamination due to pressurization or from coatings needed to arrest the loss. The military could continue to emphasize HgCdTe, which promises a more idealized solution to their needs.
- An effort be initiated to assess the effect of impurities from natural or purposeful sources on key phase diagram characteristics.
- The other thermal and atomic properties continue to have second priority for funding until more evidence for specific material selection is gathered from the phase diagram and partial pressure efforts.

C. EVALUATING CRYSTAL GROWTH MECHANIZATIONS

Understanding the crystal growth process is fundamental to producing quality crystals. Quality can be defined in several fashions; among these are:

- Large-area, somewhat thick crystals for high sensitivity uses needing large focus areas (e.g., astronomical and space sensors)
- Large-volume, rapid-growth bulk crystals for sectioning and cutting to large quantities of smaller sensors (e.g., array sensors)
- Large-area but controlled thinness crystals for high sensitivity or layering uses or for eliminating machining imperfections in preparing thin sensors
- Small-area, high perfection crystals for limited quantity uses.

The various bulk and epitaxial growth techniques discussed earlier each have advantages or disadvantages in terms of the above definitions of quality. Some of the major and new techniques of interest are listed in Table V-4, along with the major process control parameters.

TABLE V-4. EVALUATING CRYSTAL GROWTH MECHANIZATION

Major Growth Methods	Critical Control Parameters
Normal Melt	Axial Temperature Gradient
Zone Melting	Radial Temperature Gradient
Pull from Crucible	Pressure
Liquid Phase Epitaxy	Geometry Limitations
Vapor Phase Epitaxy	Concentration Gradients
Molecular Beam Epitaxy	Gravity
Diode Spattering	Annealing Cycle
Rheocasting	

Essentially the problem is one of improving size, growth interface flatness, and growth speed and process repeatability without losing compositional homogeneity and structural perfection. While we identified considerable effort in applying these techniques to a wide range of materials and applications, we have not seen much in the way of fundamental studies on the experimental and theoretical limits within each growth mechanization adopted by a particular activity. Facility diagnostics, in terms of instrumented arrays of samples with a wide range of material conductivities and specific heats and varied thermocouple junction positioning to allow extrapolation back to the uninstrumented condition, have not been seen. This may partially be due to proprietary interests. Progress appears to be generated (and progress there has been) purely empirically, by trial and error.

Three major areas of effort can be discussed for each of the generic techniques listed in Table V-4. Facility diagnostics covers the detailed assessment of specific facility geometric configurations and thermal inputs in relation to control of axial and radial temperature gradients, allowable maximum sizes and shapes, the difficulty of vapor pressure matching, rod or container motions, and the influences of special forces due to inertia or magnetic fields. This area appears to be difficult to assess due to proprietary constraints on information, but the imperfections and lack of repeatability in final products makes us believe there is much room for

improvement here. Variations in product due to changes in the input materials loaded in the apparatus are well reported but the choice of what variations to study has not followed any systematic plan identifiable from the literature we reviewed. Improved understanding of phase diagrams as discussed earlier would help guide effort in this regime. Many special problems like gravity and Marangoni forces, nonstoichiometric starting mixtures, noncylindrical growth configurations, and multilayer layups have been studied but often appear to suffer from lack of fundamental understanding of the dynamic processes in the facility utilized. Table V-5 summarizes the ongoing ternary-related growth dynamics efforts identified from References 3, 4, 5, and 6.

1. Pull from a Crucible (e.g., Czochralski)

This method is difficult at best to apply to materials with high vapor pressure (like mercury) so has not had much exposure to ternary material growth. CdTe substrates have been grown and some exploratory studies of InAsSb are under way. We recommend:

- More temperature gradient diagnostic studies in existing facilities and in modifications which allow interpolation of improvements in planar growth. NASA has some interest in the non-mercury ternaries identified earlier and might want to improve their understanding of this growth process.
- More studies of the wider variety of ternary materials potentially of interest over the full visible and infrared bandwidth, including variations in their degree of stoichiometry and in the quantity and variety of impurities and additives. NASA and the military interests potentially overlap in this area.

2. Floating Melt Zone

This area is not shown in Table V-5 since it is not easily adaptable to cope with mercury vapor pressures. Several of the ternary materials identified earlier though may be producible by the technique, and comparitive studies would be desirable to assess its potentials relative to the pull-from-a-crucible technique. We recommend that:

TABLE V-5. PARTIAL SUMMARY OF ONGOING EFFORTS IN GROWTH MECHANIZATIONS

TECHNIQUE	EMPHASIS	SPONSOR	COMPANY	MATERIAL	CO	FY80 K$
Bulk Growth	Czochralski	NASA/MSFC	Rockwell	$InAs_{1-x}Sb_x$		15
		ARPA	Rockwell	CdTe		250
		AF-OSR	Rockwell	$InAs_{1-x}Sb_x$	5 μm @ 195 K	72.2
	Bridgeman	NASA/MSFC	In-house	$Hg_{1-x}Cd_xTe$		3 my
		NASA/MSFC	Clarkson	(Interface Model)		
		Army	Rockwell	CdTe		200
		AFML	New England R.C	$Hg_{1-x}Cd_xTe$ (Flat Sided Ampules)		32
	Te Rich	AFML	HEOC	$Hg_{1-x}Cd_xTe$	13 μm	3
	Te Rich	AFML	HEOC	$Hg_{1-x}Cd_xTe$	4.3 μm	450
	Hg Rich	AFML	SBRC	$Hg_{1-x}Cd_xTe$	13 μm	2
	Hg Rich	AFML	SBRC	$Hg_{1-x}Cd_xTe$	4.3 μm	415
Liquid Phase Epitaxy	Electrocrystallization	ARPA	MIT	$Hg_{1-x}Cd_xTe$		90
	Marangoni Effects	NASA	MIT	$Hg_{1-x}Cd_xTe$		
		NASA/MSFC	Rockwell	GaAs		
	Te Rich,Open Tube Slider	AFML	HEOC	$Hg_{1-x}Cd_xTe$	13 μm	Above
	Te Rich,Open Tube Slider	AFML	HEOC	$Hg_{1-x}Cd_xTe$	4.3 μm	Above
	Hg Rich	AFML	SBRC	$Hg_{1-x}Cd_xTe$	13 μm	Above
	Hg Rich	AFML	SBRC	$Hg_{1-x}Cd_xTe$	4.3 μm	Above
	Te Rich, Isothermal	ARPA	TI	$Hg_{1-x}Cd_xTe$		250
	Te Rich, Open Tube Graphite Slider	AFML	Honeywell	$Hg_{1-x}Cd_xTe$	x=.4, .37,.29, .20	104
	Sliding Boat Scaleup	ARPA/AFML		$Hg_{1-x}Cd_xTe$		(330)
	Multilayer Demonstration	Army	In-house	CdTe, $Hg_{1-x}Cd_xTe$		9 my
Vapor Phase Epitaxy		NASA/JPL	McDonnell Douglas	$Pb_{1-x}Sn_xTe$		100
Molecular Beam Epitaxy	All glass	AF/OSR	N Carolina St. U.	$Hg_{1-x}Cd_xTe$		50
		ARPA	RISC	$Hg_{1-x}Cd_xTe$		180
	Multilayer Demonstration	Army	In-house	CdTe,$Hg_{1-x}Cd_xTe$		Above (9 my)
Diode Sputtering		AF/OSR	New Jersey I.T.	$Hg_{1-x}Cd_xTe$		40
Rheocasting		ARPA/MSO				

- Some additional facility diagnostics should be carried out at several locations to define specific limits on temperature gradients and configurations. NASA may want to participate in this as part of their interest in large size detectors for space applications.
- Some ternary material load variations also need to be investigated for comparison with the other techniques.
- This technique appears to provide the best mechanism for studying Marangoni circulation effects. NASA may want to participate in this for fundamental understanding purposes or may want to place this on lower priority basis since there are growth techniques without substantial Marangoni effects which might satisfy their needs.

3. Contained Melts (e.g., Bridgeman)

Bridgeman techniques with container ampules with carefully matched expansion coefficients have shown considerable application to the growth of mercury containing materials (see Table V-5). Diagnostics of the temperature patterns within the ampule do not appear very systematic, and good mathematical representations of the thermal and composition dynamics like that of the Clarkson effort need specific verification through carefully contrived tests. A wide variety of new ternary compounds might also benefit from this technique. The Honeywell (HEOC) and Hughes (SBRC) efforts seem fairly comprehensive, but, because of present Air Force interest in array detectors, emphasis appears to be on the Liquid Phase Epitaxy portion of their contract. New England Research Center's study of flat-sided ampules to eliminate radial dendrite growth is interesting but is not expected to show much improvement.

We recommend:

- That experiments be designed to validate the Clarkson effort or an improvement of it, and that the technique and validation concept be applied to a wider variety of heater configurations and ampule materials and sizes. NASA should participate in this process in order to better calibrate its facility.
- That this technique be used to explore the other suggested compound candidates and their binary components with volatile constituents (e.g., As or N containing). This area should be particularly of interest to NASA since the initially suggested list of candidate ternary compounds in the visible and near

infrared regimes all contain potentially volatile components (e.g., AlInAs, HgCdSe, and GaNAs). In addition, this may be the place to test the impurity and additive compositions found to be of particular interest from the phase diagram studies suggested.

4. Rheocasting

The rheocasting concepts and some variations were reported in Reference 5 from Air Force Materials Laboratory efforts in other areas. It has some interesting potentials conceptually, but will have to be evaluated material by material to see if the differential forces are significant in comparison with the more natural phenomena within the growth process. NASA might want to send someone to AFML to evaluate the potential utility of this concept.

5. Liquid Phase Epitaxy

There are many different concepts which come under this base name. Under present understanding of growth processes, this generic concept appears to have advantage over the bulk concepts in terms of material homogeneity and structural perfection. Efforts at MIT, Honeywell (HEOC), Hughes (SBRC), Texas Instruments (TI), and others (see Table V-5) have shown continual improvement in areal sizes and thickness control and in the ability to lay up multiple layers one after another. The military is considering some scale-up efforts to improve output. NASA needs to participate in this effort and could benefit from exploring its application to other materials.

We recommend:

- That effort be expended in better defining the near-surface concentration and temperature gradients inherent in the several alternative mechanizations and to improve and verify mathematical models of the facility interfaces and liquid and growth dynamics. Because of the greater immediate interest and need shown by the military, it might be better for NASA to take a secondary role in these facility diagnostics.

- It is also appropriate for NASA to explore the feasibility of growing some of the other ternary combinations of interest using these techniques.
- Multilayer applications of this technique appear to be particularly promising with appropriate lattice matching and growth conditions. NASA again might ride behind the military investment with a limited subset of materials which explore other spectral regimes of interest to NASA (e.g., for 0.4 to 3 μm use).

6. Vapor Phase Epitaxy

Vapor phase epitaxy suffers most from extreme slowness but is balanced somewhat by the potential for very defect free crystals if one of the constituents is not highly volatile relative to the others. NASA's interest in PbSnTe is perhaps warranted by their planetary mission needs. Relatively small quantities of high purity material with no significant potential for space vacuum leaching could provide appropriate sensor lifetimes without compromising the performance gains from planar array configurations. InGaSb materials might also meet this criteria. We recommend that NASA continue to explore this area for low-quantity, high-quality applications.

7. Molecular Beam Epitaxy and Diode Sputtering

Both these techniques appear to be in the exploratory feasibility phases of development with moderate Air Force, Army, and ARPA investment. We did not look at these techniques in enough depth to make recommendations.

D. ASSESSING MATERIAL PERFORMANCE FOR DETECTION APPLICATIONS

This area addresses the need to understand the quality of the crystals produced, not only in terms of their detection characteristics, but also in terms relating these properties to their molecular and structural perfection. Table V-6 lists some of the key parameters for which techniques need to be developed to provide their measurement. Many of the efforts listed in Table V-5 have some of these capabilities inherent in the company efforts to define their products. Table V-7 lists those performance

TABLE V-6. ASSESSING MATERIAL DETECTION PERFORMANCE

Performance Parameters	Diagnostic Parameters
Cutoff Wavelength	Size and Shape
Carrier Concentration	Compositional Homogeneity
Carrier Mobility	Defect Concentrations
Carrier Lifetime	Dislocation Densities
Detectivity	Dopant/Impurity Distribution

TABLE V-7. PARTIAL SUMMARY OF ONGOING EFFORT IN PERFORMANCE DIAGNOSTICS

Property Measured/ Calculated	Sponsor	Company	Material	λ_{CO}	~FY80 $K
Defect & Dopant Chemistry	NASA/MSFC	Honeywell	$Hg_{1-x}Cd_xTe$		
Raman Probe Techniques	NASA/MSFC	Athens St.	GeSe, GeTe, GaS		
Spectrographic Analysis	NASA/MSFC	In House			1 my
Laser Absorption & Gain	AF/OSR	Colo. I.T.	$Hg_{1-x}Cd_xTe$		
Auger Recombination Calculations	AF/OSR	Honeywell	$Hg_{1-x}Cd_xTe$	15-30 μm	50
Auger Spectroscopy	AF/OSR	N.J. I.T.	$Hg_{1-x}Cd_xTe$	x=.25	See Table V-5
Electron & X-Ray Diffraction	AF/OSR	N.J. I.T.	$Hg_{1-x}Cd_xTe$	x=.25	See Table V-5

diagnostic efforts which were specifically identified in References 3 through 6. The Honeywell activity on defect and dopant chemistry appears to provide an excellent start towards detailed understanding of molecular effects on electric performance. Attempts were made to understand deviations from stoichiometry, the nature of the lattice defects, the mechanisms by which dopants are incorporated and affect defects, and the thermodynamics of defects, through both experiment and theory. Special attention was given to preparation of undoped and doped samples and for measuring final atomic characteristics by as many methods as practically possible with available funding. Most of the other efforts listed in Table V-7 address particular diagnostic techniques. The lack of systematic diagnostics in this area has hindered the ability to direct changes in growth techniques in order to work around undesirable trends. Considerable effort is warranted in this area.

We recommend:

- An expansion of the type of effort initiated by Honeywell for NASA to systematically assess the products from the various growth techniques in order to aid both better selection of materials and better design of facilities to eliminate process derived inhomogeneities. Although NASA has made a good start on HgCdTe, it may be more appropriate to investigate other materials with more long-range NASA importance along the lines previously discussed.
- An effort should be made to systematically assess and categorize all the diagnostic tools for determining atomic composition and lattice imperfections. The relative value, now and potentially in the future, needs to be assessed from both performance and investment standpoints. Several concepts should be chosen for development to support both research needs and the validation concepts useful in production quality control. All who have need for repeatability and quality assurance could benefit from investment in this often-neglected aspect.

E. EVALUATING TIME DECAY IN PERFORMANCE

This area is not fully separate from the previous one but is set aside to stress its practical importance. Material losses and defect migration are the primary factors which promote performance decay in most detector materials (see Table V-8). Photon conversion is degraded by pinholing due to leaching of major constituents, by loss or migration of impurities, or by migration of defects. Current transfer efficiency is affected by defect migration and surface degradation. Material losses can come from the leaching of major constituents or due to chemical or other reactions (e.g., from sealants, glues, environmental contaminants, water or oil solubility, etc.). Some of the efforts identified in References 3 through 6 are listed in Table V-9. These reflect a rising concern with lifetime considerations. Many of the chemical and earth environmental leaching processes can be eliminated by sensible design and simple encapsulation. The mercury volatility problem may have severe implications on the practicality of civilian missions using this ternary material. This is key to the recommendations:

- That NASA carefully evaluate the volatile and chemical loss aspects of the variety of candidate ternary compounds and assess the implications of these loss mechanisms to future space-based sensor designs.
- That an effort to systematically evaluate defect migration processes be undertaken. The Army inhouse effort and the Air Force activity at McDonnell Douglas may provide an initial base for this, and more detailed study will have to be made of the variety of related interface problems being addressed in the passivation research listed in Table V-12 and in the device production efforts listed in Table V-11.

TABLE V-8. EVALUATING NATURAL DECAY IN PERFORMANCE

Material Losses	Defect Migration
Volatile Components	Free Surface Defects
Chemical Leaching	Base Material Defects
	Junction or Layering Interface Defects
	Interlayer Defect Transfer

TABLE V-9. PARTIAL SUMMARY OF ONGOING EFFORTS IN LIFETIME DECAY ASSESSMENTS

Decay/Enhancement Mechanism	Sponsor	Company	Material	λ_{CO}	~FY80 $K
Passivation Effect on Time Stability	ARMY	Inhouse	$Hg_{1-x}Cd_xTe$		5 my
Mercury Loss Effects on Time Stability	ARMY	Inhouse	$Hg_{1-x}Cd_xTe$		
Scanning EER & SPV Measurements of Lifetime Effects	ARPA	U. Ill.	$Hg_{1-x}Cd_xTe$		60
Magnetic Field Enhancement of Lifetime	AF/OSR	McDonnell Douglas	$Hg_{1-x}Cd_xTe$		53

F. PRODUCING REAL DEVICES

Although important, crystal growth is unfortunately still only one of many problem areas that contribute to the ultimate performance of a detector system. All detector crystals have to have some junctions in order to carry the current away to the next stage in signal processing, although ideally one could create multilayer material combinations which provide the various integration and correlation functions of interest along the first part of the signal processing chain. While conceptually attractive, the jump to a full multilayer device is not a trivial one. Thus, some look needs to be taken of the entire device production process in order to put the crystal growth portion in perspective. Ultimately, the total process needs to be simple and amenable to standardization of the production methodology and to automated testing, while retaining adequate performance capability and a reasonable immunity to noise. Some of the critical problems are listed in Table V-10. The sizing and cleaning process can add defects. Joining, bonding, and insulating can add defects through migration, stress chemistry, etc. Special surface passivation and joining techniques can reduce the contributions but seldom eliminate them. Thus, the starting material needs to be very good and any layering processes finely controlled if the final detector is to remain within performance specifications.

TABLE V-10. PRODUCING REAL DEVICES

Assembly Mechanics	Cost Effectiveness
Cutting and Thinning Induced Defects	Bulk Quantities
Chemically Induced Defects	Standardization
Surface Passivation	Simplicity
Multilayer Layups	Automated Validation
Junctions	

Dealing with this problem is somewhat out of scope of this effort, but we have provided Tables V-11 and V-12 to add perspective. Table V-11 lists many of the major infrared device efforts utilizing ternary compounds per References 3 through 6, and Table V-12 lists some problem-oriented investments in device stabilizations and junction research based on the same source base. We do not believe that all the funding listed is correct because of some reporting ambiguity, but the trends are basically true. The critical observations from Table V-11 are that four companies dominate the efforts and that HgCdTe dominates investment due to the potential wide range of its bandwidth coverage rather than from the comparative practicalities of the production and shelf decay of this material compared to other ternary options. Can one trade less performance for more life? NASA needs to get into this field substantially, but some studies are needed integrating the many studies of NASA sensor needs to the realities of technology.

TABLE V-11. PARTIAL SUMMARY OF ONGOING EFFORTS IN DEVICE PRODUCTION

USE	MATERIAL	SPONSOR	COMPANY	λ_{CO}	# ELEMENTS	R_oA GOAL (Ω-cm^2)	TEMPERATURE	FY80 K$
Planetary Imagers	$Pb_{1-x}Sn_xTe$	NASA/JPL						
Resource Applications Imager		NASA/GSFC						
Common FLIR Module	$Hg_{1-x}Cd_xTe$	Army	Martin M/ Honeywell	8-12 μm	32	8	77°K	200
		Army	Texas Instr.	8-12 μm				310
		Army	Hughes	8-12 μm	32	8	77°K	300
PV Detectors - Sight		Army	Hughes	3-4.2 μm	20 x 16	10	190°K	750
- Sight		Army	Honeywell	3-4.2 μm	16 x 16	7	190°K	616
- Tank		Army	Honeywell	8-12 μm	120	>5		200
- Fire & Forget		Army		3-5, 10 μm	32 x 32			550
- Optimization		AF/OSR	SBRC	5 μm			High	21
- Optimization		AF/DH	SBRC	5 μm			High	210
- MIDAS		Navy/AF/Army	Honeywell	3-5 μm		>1400		912
		Navy/AF/Army	Honeywell	8-12 μm		>55		
- Communic.		AF/DH	Hughes	14 μm				830
- Alternates	$InAs_{1-x}Sb_x$	AF/DH	Rockwell	5 μm			High	480
- Stare	InSb	Army/Navy	Rockwell	5 μm	64 x 64			275
			Hughes		32 x 32			
	$Hg_{1-x}Cd_xTe$	Army/Navy	Honeywell	8-10 μm	64 x 64			250
			Texas Instr.	8-10 μm	32 x 32			
MIS Detectors - Optimization	$Hg_{1-x}Cd_xTe$	AF/OSR	Texas Instr.	5 μm			185°K	90
- MIDAS		Navy/AF/Army	Texas Instr.	3-5(p),8-10(n)				980
- Optimization		AF/DH	Texas Instr.	5 μm			185°K	100

TABLE V-12. PARTIAL SUMMARY OF ONGOING EFFORTS IN DEVICE JUNCTIONS AND STABILIZATION

USE	MATERIAL	SPONSOR	COMPANY	λ_{CO} (μm)	R_oA GOAL (Ω-cm^2)	TEMPERATURE (°K)	~FY80 K$
Passivation Research	$Hg_{1-x}Cd_xTe$	Army	Unknown	8-14		77	75
			Inhouse				6 my
Surface Passivation for 3 μm Instability	$Hg_{1-x}Cd_xTe$	AFML		3 μm			100 K
Photochemical Deposition of Silicon Oxide	$GaAs_{1-x}Sb_x$	AFML	Hughes				144
	$Hg_{1-x}Cd_xTe$						
Ion Implant Technology	$Hg_{1-x}Cd_xTe$	ARPA	Stanford				90
Electrical & Chemical Characterization of Anodic Oxides	$Hg_{1-x}Cd_xTe$	ARPA	SBRC				100
			Stanford				100
Beam Processing Techniques	$Hg_{1-x}Cd_xTe$	ARPA	New England Research				170
Hardening of TE Stare Detectors	$Hg_{1-y}Cd_xTe$	Army			10^4	10-20°K	247
Schottky Gates on Epitaxial CCDs	CdTe, $Hg_{1-x}Cd_xTe$	Army					115

REFERENCES

1. D. Long. "Photovoltaic and Photoconductive Infrared Detectors" in Optical and IR Detectors, R. J. Keyes, ed., Springer-Verlag, Berlin, 1977.

2. I. Melngailis and T. C. Harman, Semiconductors and Semimetals, Vol. 5, R. Willardson and A. Beer, eds., Academic Press, New York, 1970,

3. National Materials Advisory Board, "Ultra High Purity Silicon, Report 356, 1980.

4. H. C. Gates et al., "Present Status of GaAs," NASA Contractor Report 3093, 1979.

5. Minutes of National Research Council Commission on Sociotechnical Systems, "Committee on Assessment of Current HgCdTe Production Technology," December 1979.

6. Second STS Science Review, Marshall Space Flight Center, April 22-23, 1979.

PERTINENT PUBLICATIONS

1. W. Bardsley et al., eds., Crystal Growth: A Tutorial Approach, North-Holland, 1979.

2. B. Bartlett et al., "Growth and Properties of $Cd_xHg_{1-x}Te$ Crystals," J. Mat. Science, 4 (1969) 266.

3. B. Bartlett el al., "The Effects of Growth Speed on the Compositional Variations in Crystals of Cadmium Mercury Telluride," J. Crys. Growth, 47 (1979) 341.

4. B. Bartlett et al., "A Study of Casting in the $Cd_xHg_{1-x}Te$ System," J. Crys. Growth, 47 (1979) 341.

5. M. M. Blouke et al., "Sensitivity Limits for Extrinsic and Intrinsic Infrared Detectors," Infrared Phys., 13 (1973) 61.

6. R. Brebrick and A. Strauss et al., "Partial Pressures of Hg(g) and Te_2(g) in Hg-Te System From Optical Densities," J. Phys. Chem. Solids 26 (1965) 98a.

7. C. Elliot, "Intrinsic Carrier Concentration in Semiconducting $Cd_xHg_{1-x}Te$ Alloys," J. Phys. D: Appl. Phys., 4 (1971) 697.

8. C. Elliot et al., "Carrier Freeze-out and Acceptor Energies in p-type $Hg_{1-x}Cd_xTe$," J. Phys. Chem. Solids, 33 (1972) 1527.

9. E. Igras et al., "Ultimate Detectivity of (CdHg)Te Infrared Photoconductors," Infrared Phys., 19 (1979) 143.

10. E. Johnson and J. Schmit, "Doping Properties of Selected Impurities in $Hg_{1-x}Cd_xTe$," J. Elec. Mat., 6 (1977) 25.

11. R. J. Keyes, ed., Optical and Infrared Detectors, Springer-Verlag, 1977.

12. R. H. Kingston, Detection of Optical and Infrared Radiation, Springer-Verlag, 1978.

13. M. A. Kinch et al., "Recombination Mechanisms in 8-14μm HgCdTe," J. Appl. Phys., 44 (1973) 1649.

14. M. A. Kinch et al., "0.1 eV HgCdTe Photodetectors," Infrared Phys., 15 (1975) 111.

15. F. A. Kroger, The Chemistry of Imperfect Crystals, Vols. 1-3, North-Holland, 1973.

16. M. Lanir et al., "EBIC Characterization of HgCdTe Crystals and Photodiodes," J. Elec. Mat., 8 (1979) 175.

17. M. Lanir et al., "Backside-Illuminated HgCdTe/CdTe Photodiodes," Appl. Phys. Letters, 34 (1979) 50.

18. D. Long, "Calculation of Ionized-Impurity Scattering Mobility of Electrons in $Hg_{1-x}Cd_xTe$," Phys. Rev., 176 (1968) 923.

19. D. Long, "Uniformity of Infrared Detector Parameters in Alloy Semiconductors," Infrared Phys., 12 (1972) 115.

20. H. Matare, Defect Electronics in Semiconductors, Wiley-Interscience, 1971.

21. J. M. Pawlikowski and P. Becla, "Some Properties of Photovoltaic $Cd_xHg_{1-x}Te$ Detectors for Infrared Radiation," Infrared Phys., 15 (1975) 331.

22. J. Schmit and C. Speerschneider, "Phase Diagram of $Hg_{1-x}Cd_xTe$," Infrared Phys., 8 (1968) 247.

23. J. Schmit and E. Stelzer, "The Effect of Annealing Temperature on the Carrier Concentration of $Hg_{0.6}Cd_{0.4}Te$," J. Elec. Mat., 7 (1978) 65.

24. J. Schmit and J. Bowers, "LPE Growth of $Hg_{0.6}Cd_{0.40}Te$ From Te-Rich Solution," Appl. Phys. Letter, 35 (1979). 457.

25. W. Scott and R. Hager, "Anomalous Electrical Properties of p-Type $Hg_{1-x}Cd_xTe$," J. Appl. Phys., 42 (1971) 803.

26. W. Scott et al., "Electrical and Far-Infrared Optical Properties of p-Type $Hg_{1-x}Cd_xTe$," J. Appl. Phys., 47 (1976) 1408.

27. W. Scott, "Electron Mobility in $Hg_{1-x}Te$," J. Appl. Phys., 43 (1972) 1055.

28. A. Strauss and R. Brebrick, "Vapor-Crystal Equilibrium and Electrical Properties of HgTe," J. Phys. Chem. Solids, 31 (1970) 2293.

29. W. Shockley and W. T. Read, Jr., "Statistics of the Recombinations of Holes and Electrons," Phys. Review, 87 (1952) 835.

30. O. Tufte and E. Stelzer, "Growth and Properties of $Hg_{1-x}Cd_xTe$ Epitaxial Layers," J. Appl. Phys., 40 (1969) 4559.

31. P. Vohl and C. Walfe, "Vapor Phase Growth of $Hg_{1-x}Cd_xTe$ Epitaxial Layers," J. Elec Mat., 7 (1978) 659.

32. R. K. Willardson and A. C. Beer, eds., Semiconductors and Semimetals, Vol. 5, Infrared Detectors, Academic Press, 1970.

33. R. K. Willardson and A. C. Beer, eds., Semiconductors and Semimetals, Vol. 12, IR Detectors II, Academic Press, 1977.